Influence of neotectonics on land surface evolution in the upper part of the Blue Nile Basin (Ethiopia): findings from a DEM

Michal Kusák[1,*], Vít Vilímek[2], Jozef Minár[3]

[1] Institute of Rock Structure and Mechanics of the Czech Academy of Sciences, Czech Republic
[2] Charles University, Faculty of Science, Department of Physical Geography and Geoecology, Czech Republic
[3] Comenius University in Bratislava, Faculty of Natural Sciences, Department of Physical Geography and Geoecology, Slovak Republic
[*] Corresponding author: kusak@irsm.cas.cz

ABSTRACT

The morphometric analysis of lineaments, valleys and signs of erosion taken from a digital elevation model (DEM) made it possible to not only confirm most of the conclusions of the morphotectonic development of the Blue Nile Basin from the previously published results of structural, petrological, tectonic and geochronological analyses, but also to expand our knowledge by applying several new hypotheses. The relative age of the morpholineaments of particular directions was estimated from the character of topographic profiles. Faults, lineaments and valleys are predominantly oriented in a direction compatible to the published concepts of the tectonic development of the area. Overall, the most abundant NE-SW and NNE-SSW lines reflect a change of extension from a NW-SE to WNW-ESE direction during the Pliocene, in relation to the creation and development of the Main Ethiopian Rift (MER). This is confirmed by a more developed character of the valleys and less pronounced erosion activity of the NE-SW oriented valleys contrary to the deeper narrower NNE-SSW valleys characterised by downward and headward erosion in the second direction. The most pronounced morphological manifestations of the E-W extension of the MER and western Afar during the Quaternary are confined to the borders of the MER. The directions of the Pre-Neogene rift structures to the NW-SE and WNW-ESE are compatible with the oldest elements of the current landscape and with the relict fragments of the valley network on the SE boundary of the upper Blue Nile Basin, which could have been drained across current shoulders of the MER to the S and E before the Late Miocene.

KEYWORDS

landscape evolution; neotectonics; river piracy; lineaments; DEM; Main Ethiopian Rift; Ethiopian Highlands

Received: 17 April 2019
Accepted: 28 June 2019
Published online: 26 August 2019

Kusák, M., Vilímek, V., Minár, J. (2019): Influence of neotectonics on land surface evolution in the upper part of the Blue Nile Basin (Ethiopia): findings from a DEM. AUC Geographica 54(2), 129–151
https://doi.org/10.14712/23361980.2019.13

1. Introduction

Lineaments are linearly arranged elements of the landscape – linear sections of a valley, ridges or straight sections of slopes – should be considered as a potential zone of brittle fractures of bedrock and/or the concentration of erosion processes with an influence on the geomorphological evolution of an area (Abdullah et al. 2010). An analysis of the lineaments can give an insight into landscape evolution, thus providing information on tectonic activity over large areas, which is particularly useful for areas with limited field access (Ehlen 2004), like the Ethiopian Highlands. Recently, the lineaments are increasingly used not only as a surface expression of individual faults (fracture zones) but their statistics is used also to define/confirm the character (directions) of the palaeomorphotectonic stress fields (Minár and Sládek 2008; Koronovskya et al. 2014; Šilhavý et al. 2016).

In this paper we aim to understand relations between landforms and the tectonic structures of the Ethiopian Highlands, as the region is strongly influenced by tectonics (Kazmin 1975; Pik et al. 2003; Beyene and Abdelsalam 2005; Gani and Abdelsalam 2006; Gani et al. 2007, 2009; Wolela 2010). We focused on the upper part of the Blue Nile Basin.

The main objectives of this work are to: 1) analyse the morpholineaments, faults and valley networks of the Blue Nile Basin and their interrelationships; 2) study the relation between the morpholineaments and the geomorphological evolution, in order to determine which elements are potential zones of brittle fractures of bedrock and serve as concentrations for erosion processes; 3) identify areas with the most dynamic changes of valley networks.

Several works deal with the tectonic and volcanic history of the upper part of the Blue Nile Basin (Abebe et al. 1998; Chorowicz et al. 1998; Wolfenden et al. 2004; Pik et al. 1998, 2003; Kieffer et al. 2004; Gani et al. 2009); however, less attention has been paid to the related geomorphic development. Local morphotectonic and morphodynamic aspects have mainly been investigated (Ayalew and Yamagishi 2003; Ismail and Abdelsalam 2012; Kusák et al. 2016; Mäerker et al 2016; Kycl et al. 2017; Gani and Neupne 2018). Works by Gani and Abdelsalam (2006) and Gani et al. (2007) deal most comprehensively with the selected aspects of geomorphic development.

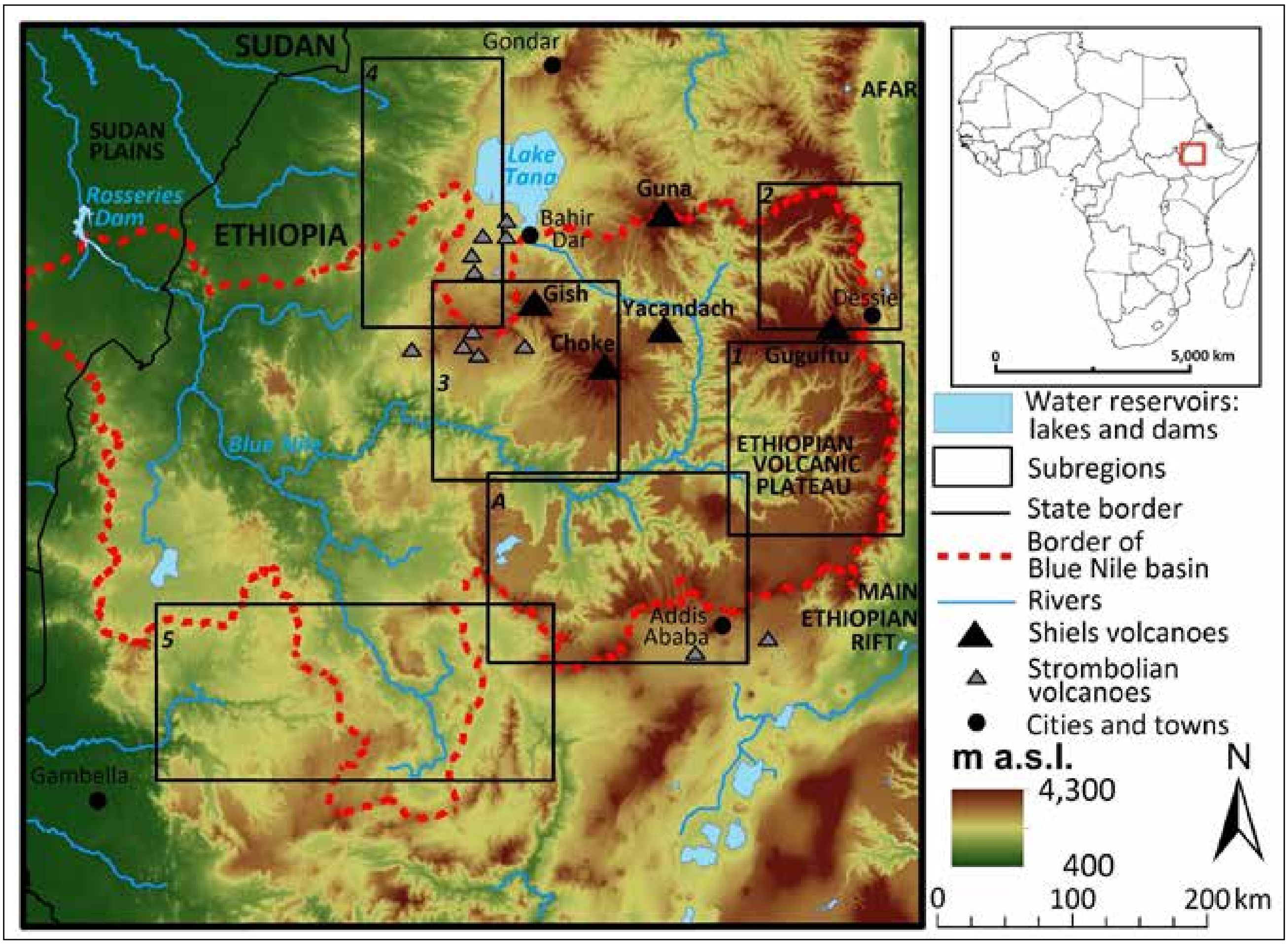

Fig. 1 Map of the Blue Nile basin and adjacent area, Ethiopian Highlands. Subregions particularly analyzed in the following text: 1 – the Jemma River; 2 – Beshlo Wenz River; 3 – Volcanoes Mt. Choke and Mt. Gish; 4 – Lake Tana; 5 – Didessa River and Baro River; A – Guder River and Muger River.

They refuse the older idea that present physiography of the elevated plateau exists since the Oligocene (e.g. Pik et al. 2003) and they argue that the rapid increase of incision rate of the Blue Nile initiates ca. 10 Ma ago. This paper presents evidence from satellite data that support young (Late Miocene – Quaternary) increasing morphotectonic activity of the territory, specifying directions and space impact of palaeomorphotectonic fields on the land surface development.

2. The study area: geomorphological and geological settings

The study area includes the Blue Nile Basin between Lake Tana and the Roseires water reservoir (175,400 km^2) and the adjacent area (Figure 1). The Blue Nile Basin consists of a large plateau that is inclined from the border of Afar and the MER (more than 3,000 m a.s.l.) to the W and NW (approximately 2,000 m a.s.l.). Huge Neogene shield volcanoes tower up to 2,000 m above the plateau, and smaller strombolian Quaternary volcanoes are concentrated to the SSW of Lake Tana reach several hundreds of meters at most (Kieffer et al. 2004). Pliocene and Quaternary tectono-thermal uplift of the rift shoulders and a swell centred on the Lake Tana basin are responsible for the recent elevation of the plateau (Chorowicz et al. 1998; Ismail and Abdelsalam 2012; MacGregor 2015; Gani and Neupne 2018). Uplift caused the rivers to cut into the bedrock and divide the area by canyons and deep valleys with steep slopes linked to faults in the eastern part of the study area (Gani et al. 2009). An older landscape area at a lower elevation and with gentle valley slopes is situated in the western part of the study area and the Blue Nile flows through the basin with a low vertical division (Figure 1).

The modern topography of the area formed Tertiary and Quaternary volcanism and tectonics. The uplift of the Ethiopian Highlands (during the last 29 Ma) and opening of the MER (during the last 18 Ma) has led to the formation of faults and cracks (Kazmin 1975; Pik et al. 2003; Beyene and Abdelsalam 2006; Gani et al. 2007; Gani et al. 2009; Wolela 2010; Ismail and Abdelsalam 2012).

The plateau in the eastern part of the study area is built by various types of Cenozoic volcanic rocks and several Cenozoic volcanoes tower above it. Erosion by the Blue Nile and its tributaries exposed Jurassic and Crateceous sedimentary complexes in the valleys incised into the plateau. The western part of the study area is built by a Precambrian crystalline complex and volcanics (Figure 2; Mangesha et al. 1996).

The Ethiopian Highlands are marked by a number of faults increasing from the west to the east, where they border the MER – part of the East African Rift (Chorowitz 2005). The oldest Permo-Trias and Crateceous-Palaeogene rift systems in the study area have a NW-SE orientation (Gani et al. 2009; MacGregor 2015). The main phase of extension in the MER started approximately 11 Ma (Ukstins et al. 2002) and the majority of fault activity occurred in the last 5–9 Ma, and particularly in the last 1–2 Ma (MacGregor 2015). The NW-SE Late Miocene extension formed NE(NNE)-trending faults (Wolfenden et al. 2004; Gani et al. 2009). E-W and NNE-SSW Quaternary extensions

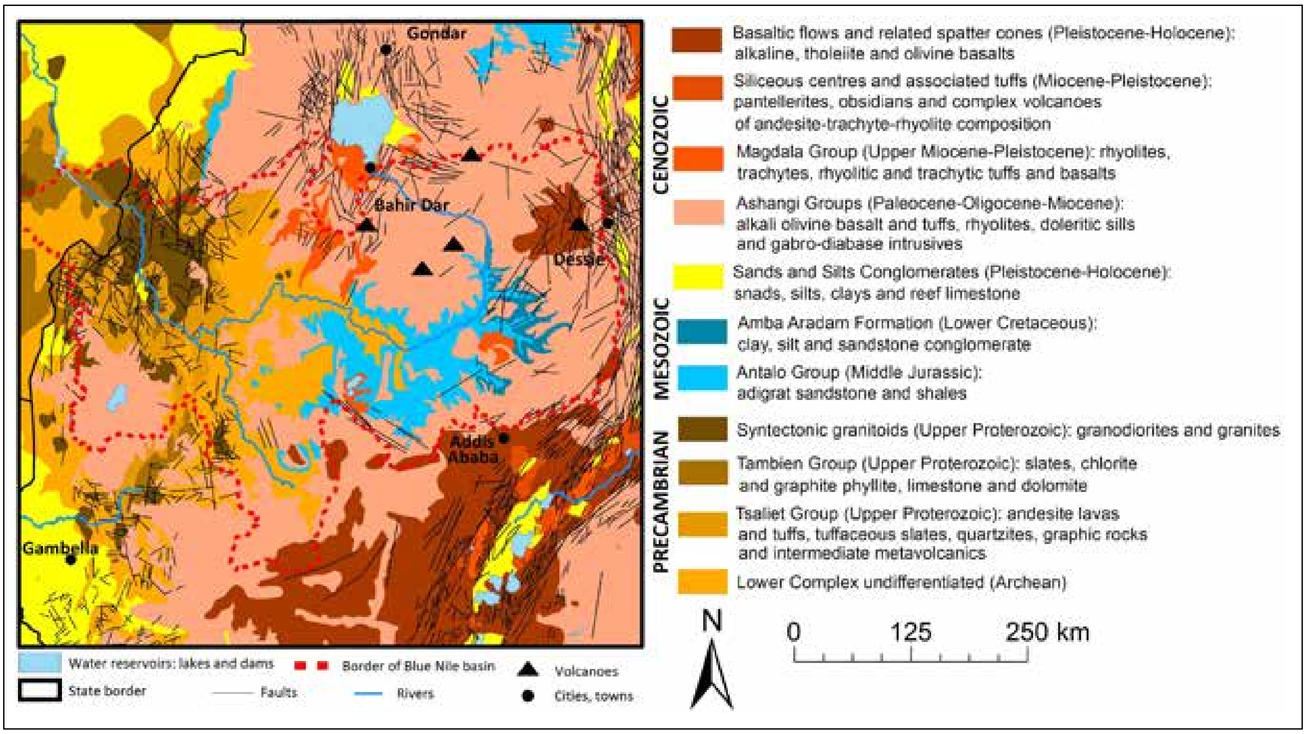

Fig. 2 Geological map of the Blue Nile basin and adjacent area, Ethiopian Highlands (scale 1 : 250,000; after Mangesha et al. 1996).

opening the MER are related to the development of E-trending transverse faults. N-ESE- and NW-trending extensional structures are connected with the NE-SW Quaternary extension in southern Afar and the E-W extension in western Afar (Gani et al. 2009). To the west of Addis Ababa, an elongated Yerer-Tullu Wellel volcano-tectonic lineament is probably an inherent structure, which has decoupled the Northern Ethiopian Plateau and the MER as a transtensional dominantly oblique E-W to ENE-WSW structure since the Late Miocene (Abebe et al. 1998).

3. Materials and methods

3.1 Digital Elevation Model (DEM) and satellite images

In this paper we use the SRTM DEM 1 Arc-Second Global version (resolution ≈ 30 m), which was released in September 2014. Shaded relief images with varying directions of illumination were created in ArcMap 10.2 (ESRI 2015) using the hillshade tool (Spatial Analyst Toolbox → Surface toolset). Various elevation angles of the illumination source (30°, 35°, 40° and 45°) and four different values of illumination azimuth 1) from the north (solar azimuth of 0°), 2) from the north-east (solar azimuth of 45°), 3) from the east (solar azimuth of 90°), and 4) from the south-east (solar azimuth of 135°), were used in order to assure the independency of the results from the direction of illumination. This procedure maximizes the visualization of a surface for better observation and graphical display, to allow for the extraction of lineaments by using shaded-relief process by changing the illumination azimuth (Smith and Clark 2005; Ahmed et al. 2017).

3.2 Analysis of linear features

In the selected areas of the Ethiopian Highlands we mapped the linearly arranged elements of the landscape, for example linear sections of valleys, ridges or straight sections of slopes. These linear landforms and structures were manually mapped from: a) digital elevation model (hillshade images of various elevation angles of the illumination source and solar azimuths), and b) satellite images of Google Earth (pixel size of 15 m, scale 1 : 100,000), and subsequent overlapping of the layers (according to Wladis 1999; Ehlen 2004).

Many of these long linear structures are parallel to each other and the processes forming the current landscape are concentrated there. In order to determine whether certain parallel linear structures are of the same age and were created by the same process (tectonic activity and erosion), the parallel mega-lineamentswere marked with the same colour (red, green, blue, etc.). The shortest length of the mega-lineamentswas 20 km. Shorter linear structures (length < 20 km) are called lineaments and thousands of them are seen on the Ethiopian Highlands. We mapped the linearly arranged elements of the landscape (the mega-lineamentsand lineaments) for an analysis of the main directions of the landscape forming processes. The faults in the Ethiopian Highlands were taken from the geological map of Ethiopia (scale 1 : 250,000; Mangesha et al. 1996).

A valley network model for the Ethiopian Highlands was extracted from SRTM DEM by following method of Jenson and Domingue (1988) and using ArcHydro tools in ArcGIS 10.2.: *Fill* → *Flow Direction* → *Flow accumulation* (ESRI 2015), i.e. the valley network was identified by analysing the flow accumulation after a filling function that was applied to remove sink-like artefacts caused by noise and inaccuracies in the original DEM dataset. The threshold of contributing area for the valley network generation was 1,000 pixels (0.9 km^2). For the analysis of the azimuth of stream channels, we converted the valley network raster into a vector format.

The azimuths of megalineaments, lineaments, and faults were determined in terms of the orientation of lines to the coordinate system and the azimuth of stream channels was also determined as the orientation of the stream channels (i.e. parts of valleys from the valley heads to the first point of the valley confluence; or parts of valleys between two valley connection points) to the coordinate system. The azimuths were illustrated by rose diagrams, which are divided into 72 intervals of 5° (360° in total). The numbers of lines in the rose diagrams were multiplied (weighted) by their length according to Belisario et al. (1999), Ciotoli et al. (2003) and Kusák et al. (2016).

Moreover, several types of profiles were created: 1) valley cross-sections which are in figures depicted by different colours (e.g. green, red) to determine the erosion intensity and (if possible) the relative age; 2) long profiles in the landscape to reveal the possibilities of river piracy; 3) profiles perpendicularly to the MER margin to reveal its block structures.

4. Results

4.1 Aggregated characteristics

In the eastern part of the Blue Nile Basin the old plateaus are strongly eroded by fluvial erosion and they recede in favour of expanding deep valleys. The fragments of the plateaus consist of Paleocene-Oligocene-Miocene basalts and tuffs and deeply cut valleys are also located there. In the western part of the Blue Nile Basin, Precambrian rocks are exposed (Figure 2).

A total of 161 mega-lineaments(with an average length of 60 km), 1,264 faults (with an average length of 21 km), 3,429 lineaments (with an average length of 10 km) and 81,137 valleys segments (with an average length of 2.3 km) were mapped and analysed in the upper part of the Blue Nile Basin. The results were then compared using azimuths and rose diagrams (Figure 3). The analysis revealed that the mega-lineaments(Figure 3A,B) and faults (Figure 3C, D) are strongly correlated and concentrated into two directions: azimuth 20° (NNE-SSW orientation; red lines in Figure 3A) and azimuth 40° (NE-SW orientation; green colour in Figure 3A). The third-most dominant direction being E-W (azimuth 90°) is clearly visible in the lineaments. It has not a significant reflection in mapped faults, however Abebe et al. (1998) and Gani et al. (2009) also mentioned important faults of this direction. Smaller concentrations of linear features were also identified in the following directions: ENE-WSW (azimuth 80°; blue lines), WNW-ESE (azimuth 115°; brown lines), NW-SE (azimuth 145°; orange lines), NNW-SSE (azimuth 170°; violet lines) and N-S (azimuth 0°, black lines). Not all these directions are clearly reflected in aggregated faults but can have a fault reflection at a local level.

4.2 Local scale analysis

The sub-regions 1–5 from Figure 1 were chosen in order to represent various types of landscapes in the upper part of the Blue Nile River Basin. Sub-regions 1 (covering the area of 18,800 km^2) and 2 (11,500 km^2) are on the boundary of the Ethiopian Highlands close to the MER. Sub-region 3 (20,500 km^2) is a typical area

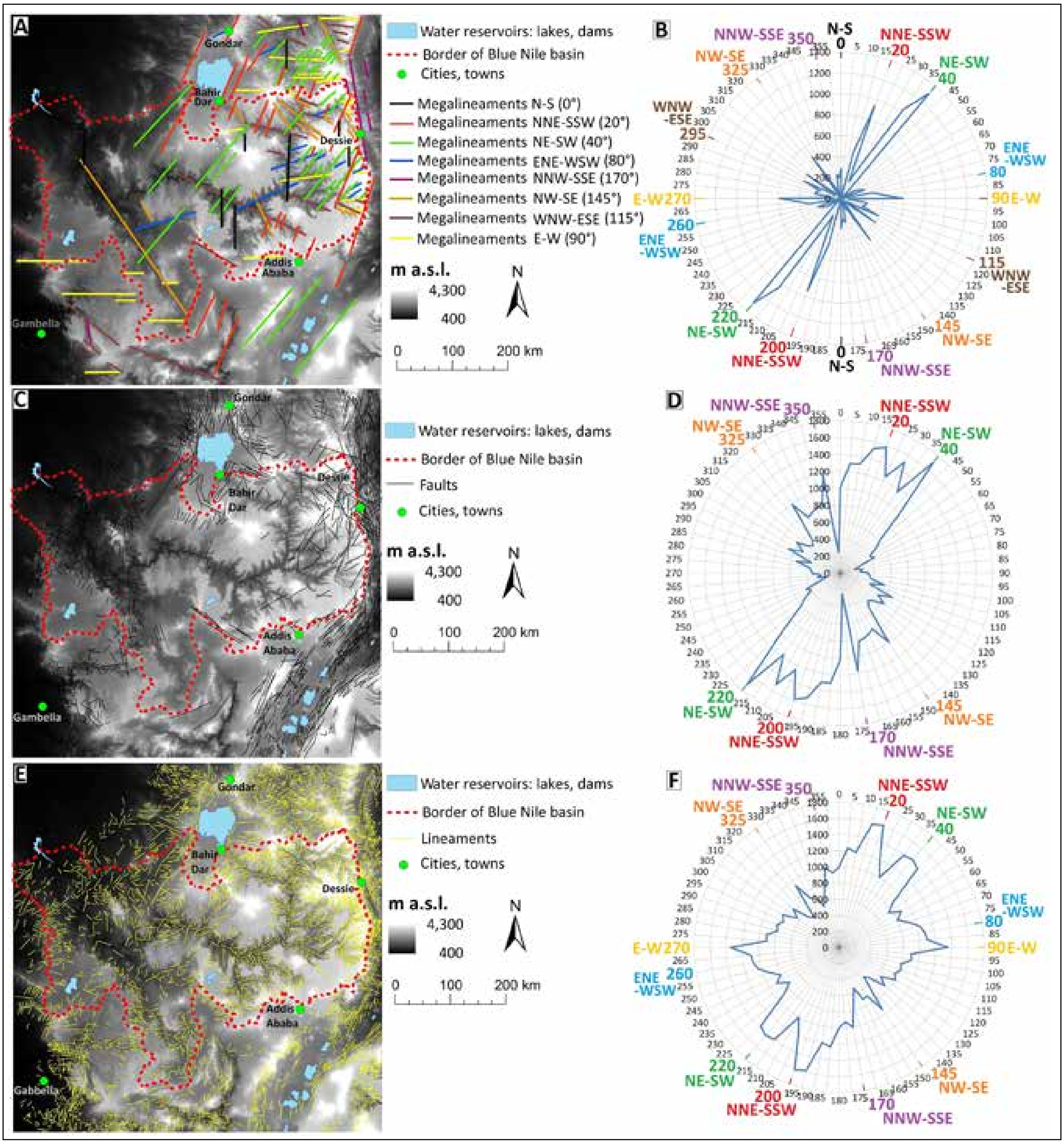

Fig. 3 A) Map of megalineaments; B) rose diagram of megalineaments; C) map of faults; D) rose diagram of fault azimuths; E) map of lineaments; F) rose diagram of lineament azimuths.

adjacent to the central volcano, while sub-region 4 (21,000 km^2) represents the Lake Tana area. Sub-region 5 (35,000 km^2) in the southwest represents a highly-eroded part (i.e. the lowest part) of the Ethiopian Highlands.

It is evident that the NE-SW direction (green lines) is important in the sense of the valley evolution. This is true across all of the sub-regions, regardless of the type of relief, and could represent an old structural predisposition, which influenced the valley network evolution in the Ethiopian Highlands.

4.2.1 The Jemma River

The local scale analysis of sub-region 1 in the catchment of the Jemma River revealed that apart from the importance of the NE-SW orientation (azimuth 40°;

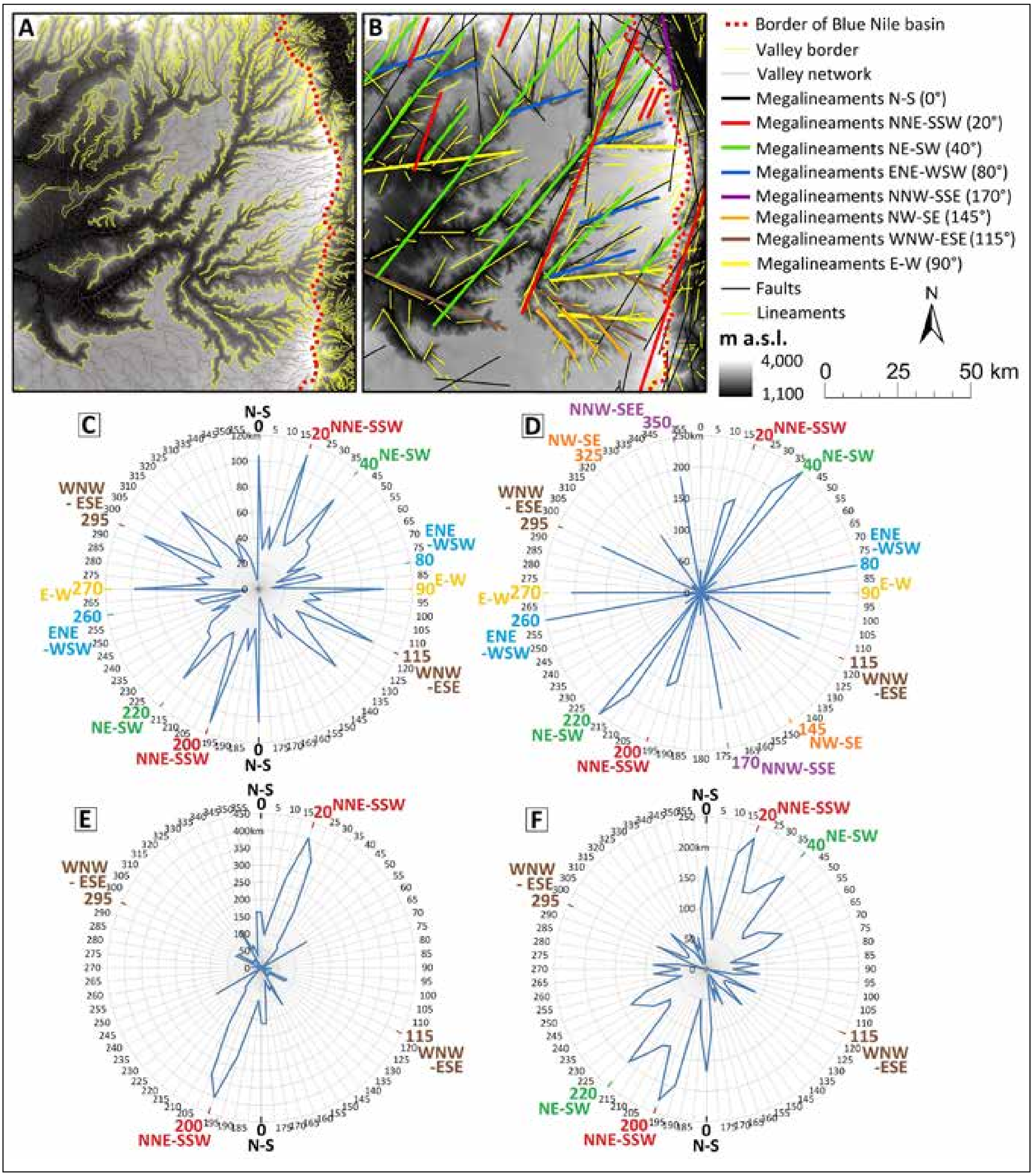

Fig. 4 The sub-region 1 (Jemma River Basin sub-region): A) map of the valley network and valley border; B) map of megalineaments, faults and lineaments; C) rose diagram of valley network azimuths; D) rose diagram of mega-lineamentsazimuths; E) rose diagram of fault azimuths; F) rose diagram of lineament azimuths.

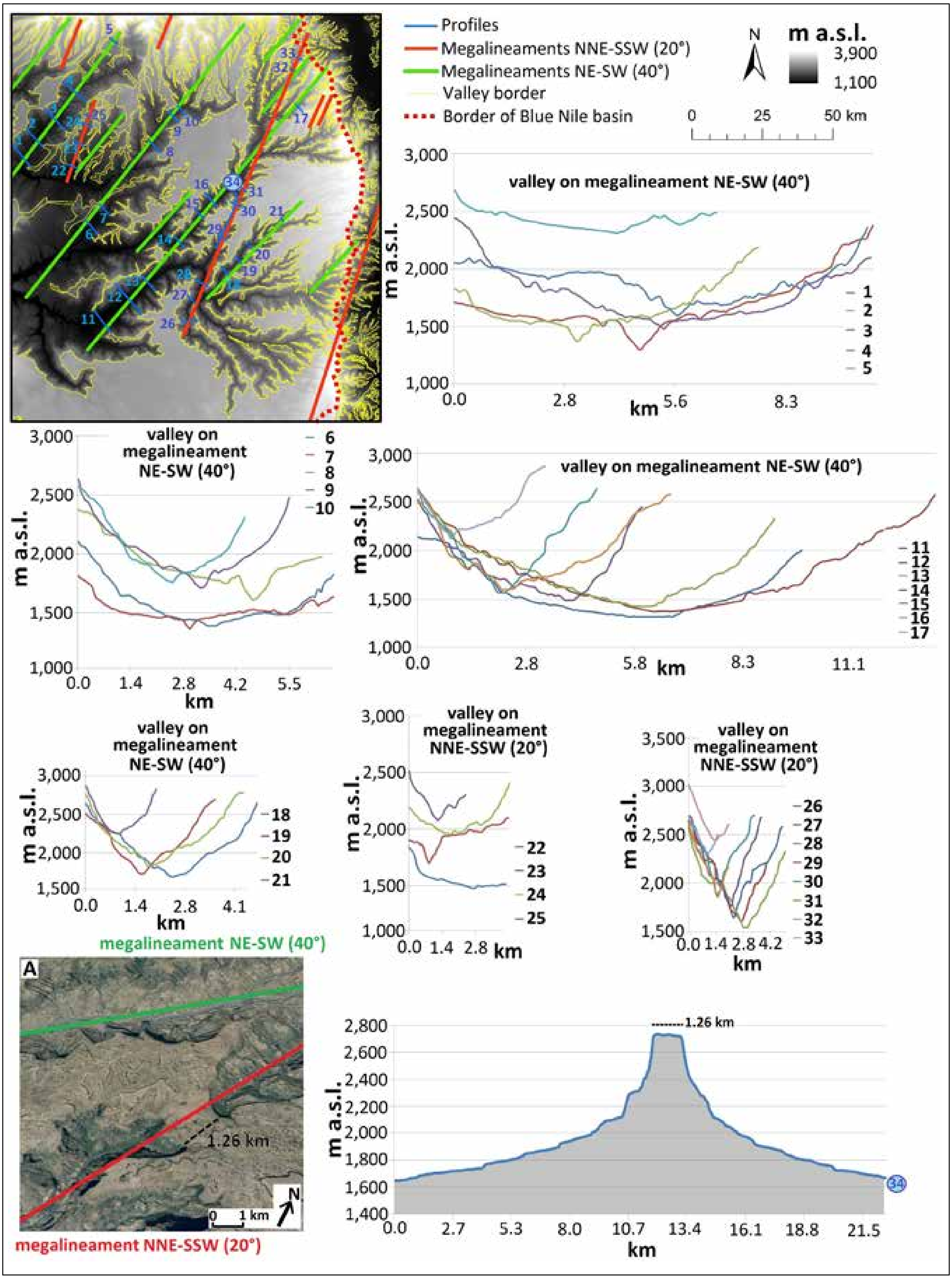

Fig. 5 Profiles in sub-region 1 (Jemma River Basin). Profiles 1–21 are valley cross-sections across green lines and profiles 22–33 are valley cross-sections across red lines; A – longitudinal profile No. 34 along a single red line (a site with a tendency for river piracy).

green line), the NNE-SSW orientation (azimuth 20°; red line) plays a more significant role in the valley network evolution and lineament depiction. The rose diagram for the faults suggests tectonic predisposition. Both directions (green and red) have a similar azimuth (40° and 20°, respectively); however, they are sharply bounded and distinguished in the rose diagrams (Figure 4). The shapes of the red line valley cross-sections suggest more intensive downward erosion compared to the green line valley cross-sections, which suggests that the red line direction is younger (Figure 5). One site with a tendency to river piracy was also positively identified along one of the red lines (Figure 5A). The headward erosion is strong

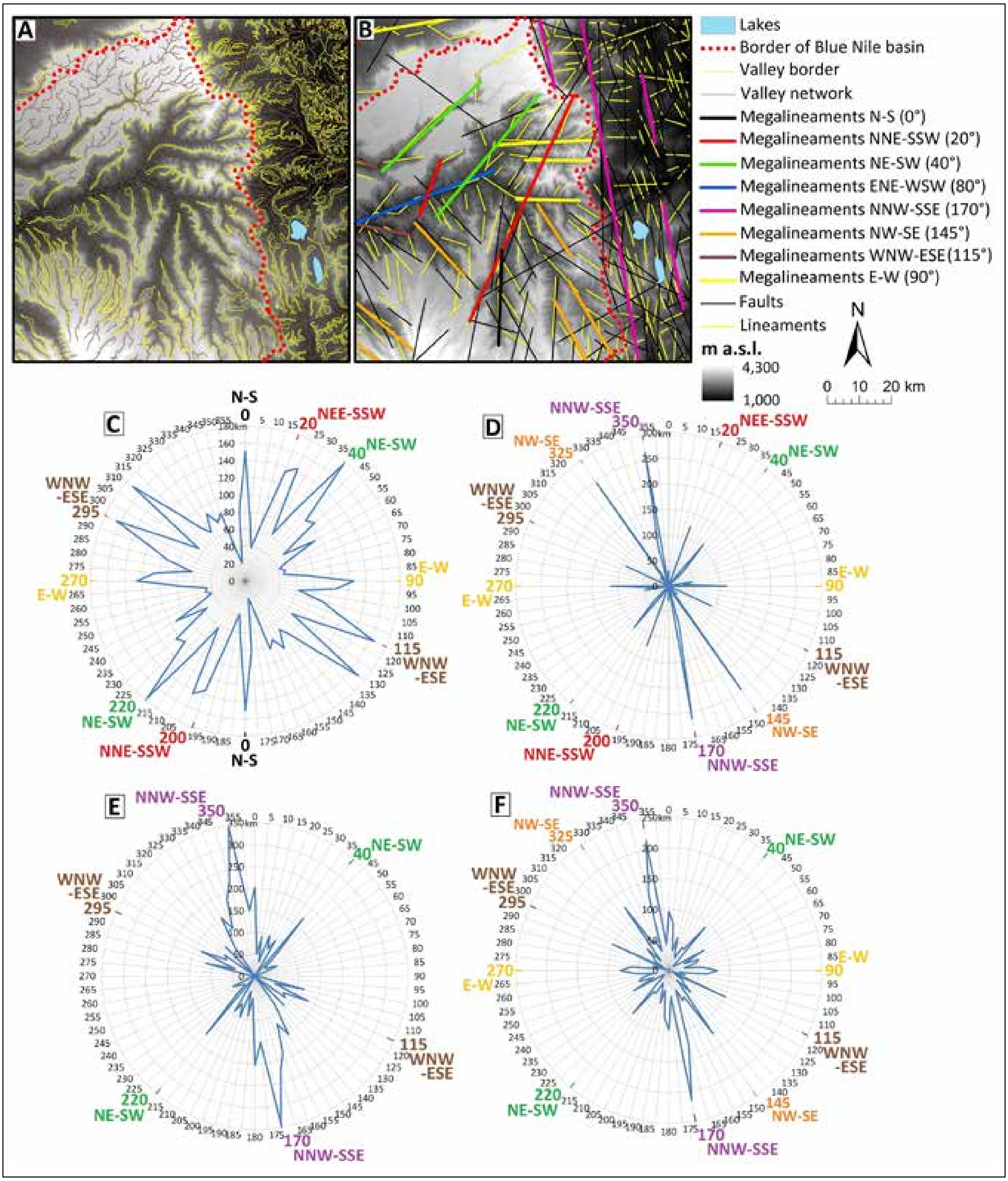

Fig. 6 Sub-region 2 (Beshlo Wenz River Basin sub-region): A) map of the valley network and valley border; B) map of megalineaments, faults and lineaments; C) rose diagram of valley network azimuths; D) rose diagram of mega-lineamentsazimuths; E) rose diagram of fault azimuths; F) rose diagram of lineament azimuths.

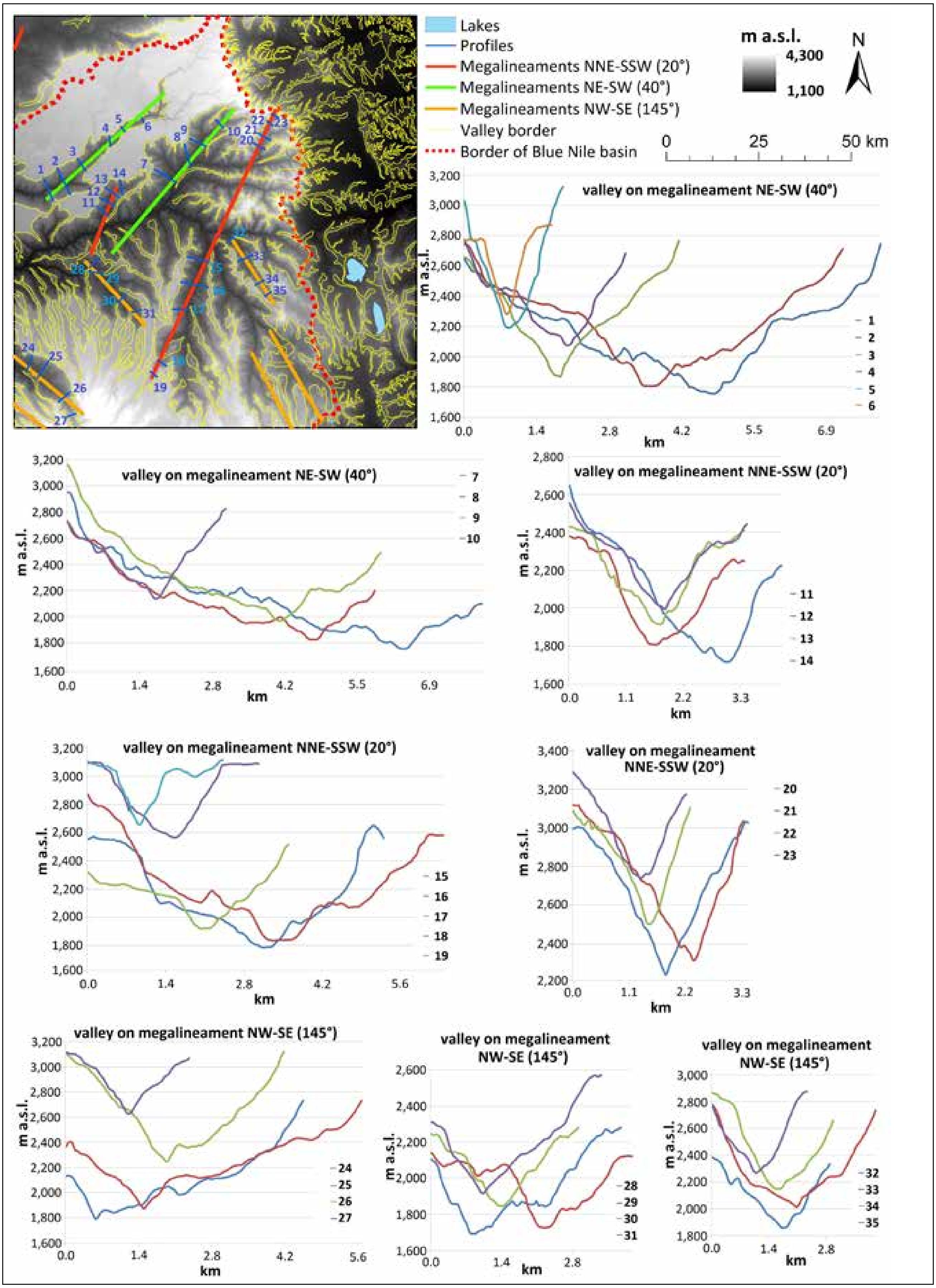

Fig. 7 Profiles in the Beshlo Wenz River Basin sub-region. Note: Profiles 1–10 are cross-sectional profiles directed across the valley marked by green lines; and 11–23 are cross-sectional profiles directed across the valley marked by red lines. Profiles 24–35 are cross-sectional profiles directed across the valley marked by an orange line.

from both sides of the two different valleys and river piracy can be expected to happen soon because the remnant of the original relief created by the basalt layer is only 1.3 km wide.

It is clear that the shape of the cross-sectional profile is influenced by several processes (or predispositions), including intensity and type of erosion, discharge and lithology; nevertheless, the set of profiles will reveal the general trend in valley evolution (if the lithology is homogeneous), which can be compared to other sub-regions. Valley cross-sections along the green lines (profiles 1–21 in Figure 5) are wider and more open compared to the profiles along the red lines (especially profiles 26–33), which are more narrow and tighter. This is regardless of the position of the valley in the river network system i.e. profiles of one direction are similar in the upper, middle and lower parts of the valley system.

4.2.2 Beshlo Wenz River

The valley network predisposition of the landscape evolution in the Beshlo Wenz Basin (sub-region 2) is similar to the Jemma River Basin. However, the faults do not have an azimuth of 20°, but the NNW-SSE orientation (azimuth 170°; violet colour on the graphs) is well pronounced (Figure 6). The Afar area adjacent to the Blue Nile Basin, is also included in this sub-region. The Rift has a NNW-SSE direction herein. Border faults (violet colour) are reflected in lineaments and megalineaments. The rose diagram for the valley network is rather complex because the western part is similar to sub-region 1 (Jemma River Basin), while the eastern part bears significant features of the slope facing the MER.

In accordance with sub-region 1, the valleys in the Beshlo Wenz catchment lying along green lines, are again more open and wide, while those running along the red lines are markedly incised (Figure 7). The only exceptions are profiles 3 through 6, and 10 (closest to the rift, Figure 7), which are also very narrow like those connected to the red lines. The area next to the border of the MER is under very intensive young evolution (strong downward erosion) regardless of the type of valley (red or green lines).

Several tectonic blocks evolved on the east-facing slope of the rift, which are asymmetrical in their cross-sectional profile and retain small lakes (Figure 8). The drainage in a NNW-SSE orientation is modified by strong headward erosion along the steep, east-facing fault slope. In our fieldwork, we identified the case of

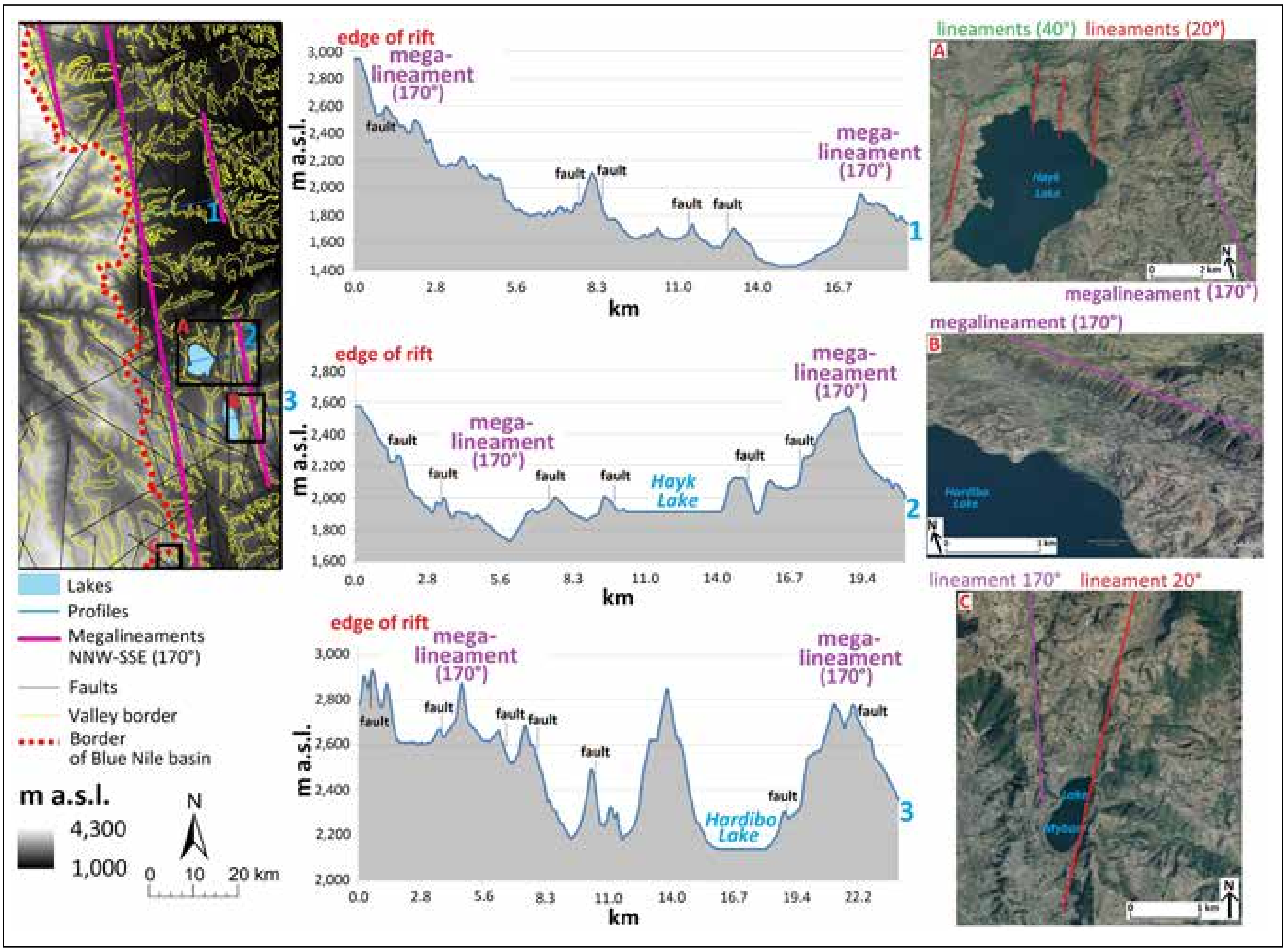

Fig. 8 Cross-sectional profiles oriented towards the MER. Tectonic blocks, which are asymmetrical in the cross-sectional profiles evolved here and retain Lake Hayk (A), Lake Hardibo (B) and Lake Mybar (C).

Lake Mybar (Figure 8C) – the lake is drained to the east nowadays because a small river reached the lake shore due to very intensive headward erosion and the former drainage to SSE was abandoned.

In this locality the tectonic predisposition is represented by faults with an azimuth of 20°. This is also the area with highest frequency of faults. Nevertheless, 30 km to the north the tectonic predisposition is changing in connection with the main structures of the rift. Lake Hardibo (Figure 8B) is predisposed by tectonics with an azimuth of 170° (NNW-SSE orientation) depicted by a violet colour in Figure 6 and 8, while in the surrounding of the adjacent Lake Hayk (Figure 8A) both NNE-SSW and NNW-SSE trending faults were identified (red and violet lines, respectively).

4.2.3 Volcanoes Mt. Choke and Mt. Gish

The situation around the volcanoes of Mt. Choke (4,100 m a.s.l.) and Mt. Gish (2,890 m a.s.l.) is rather

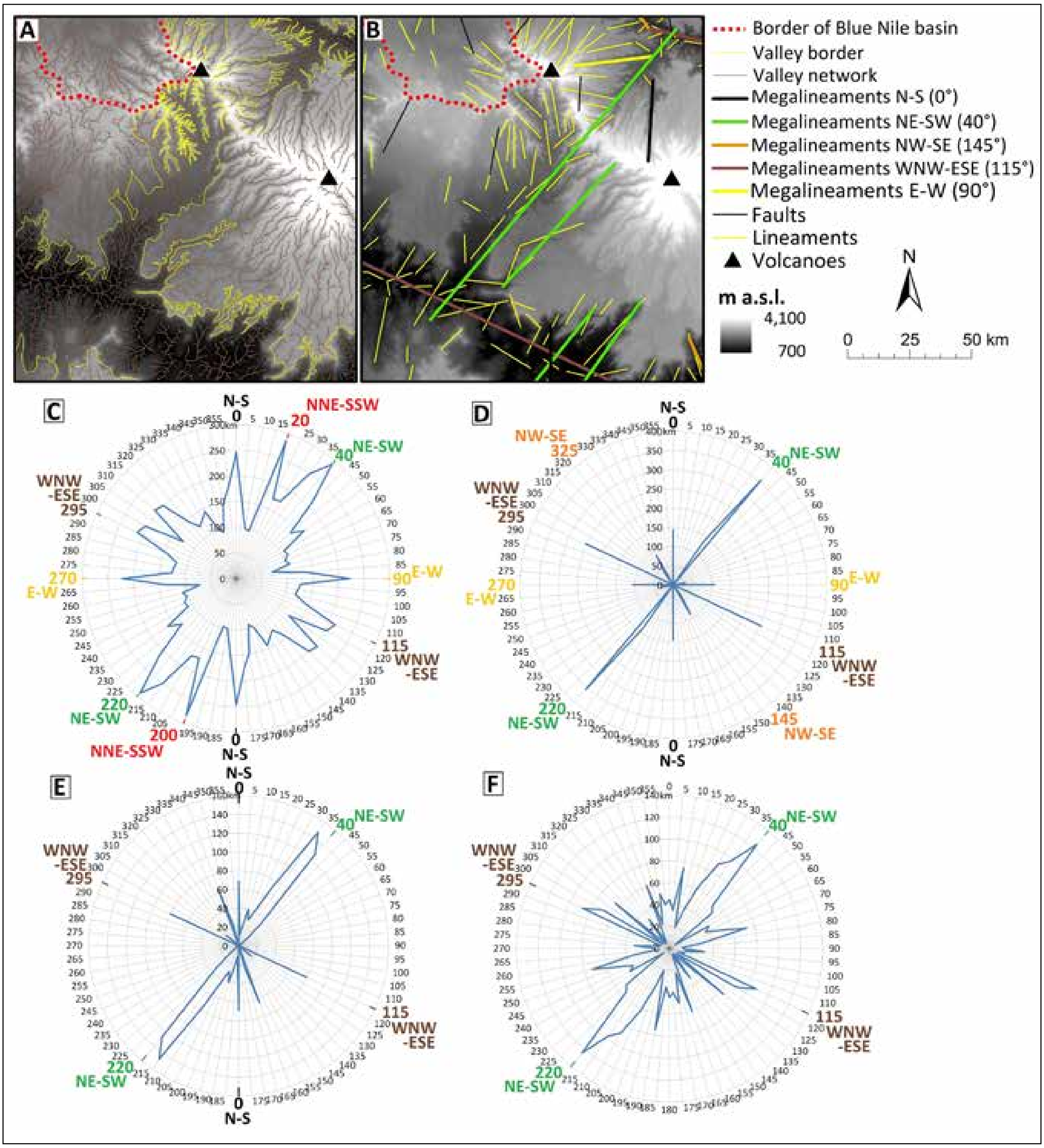

Fig. 9 Sub-region 3 (Mt. Choke and Mt. Gish volcano sub-region): A) map of the valley network and valley border; B) map of mega-lineaments, faults and lineaments; C) rose diagram of valley network azimuths; D) rose diagram of mega-lineaments azimuths; E) rose diagram of fault azimuths; F) rose diagram of lineament azimuths.

simple. The valley system reflects the position of the volcanoes in this sub-region (radial network with preferences towards certain directions); nevertheless, all other rose diagrams show NE-SW trending faults, lineaments and mega-lineamentswithout any influence of the younger NNE-SSW tectonics (Figure 10).

The long valley system between the volcanoes of Mt. Choke and Mt. Gish is probably a part of an older river network, which is pronounced in this part of the Ethiopian Highlands due to the NE-SW trending mega-lineaments identified in all of the sub-regions (Figure 10). Position on the boundary between the LT and HT provinces of flood basalts (Pik et al. 1998; Kieffer et al. 2004) could also play a role. However, parallel to this NE-SW oriented valley, a younger, deeper and narrower valley has been created on the lower slopes of Mt. Choke, which were dated by Kieffer et al. (2004) to an age of 22.4 Ma. This direction

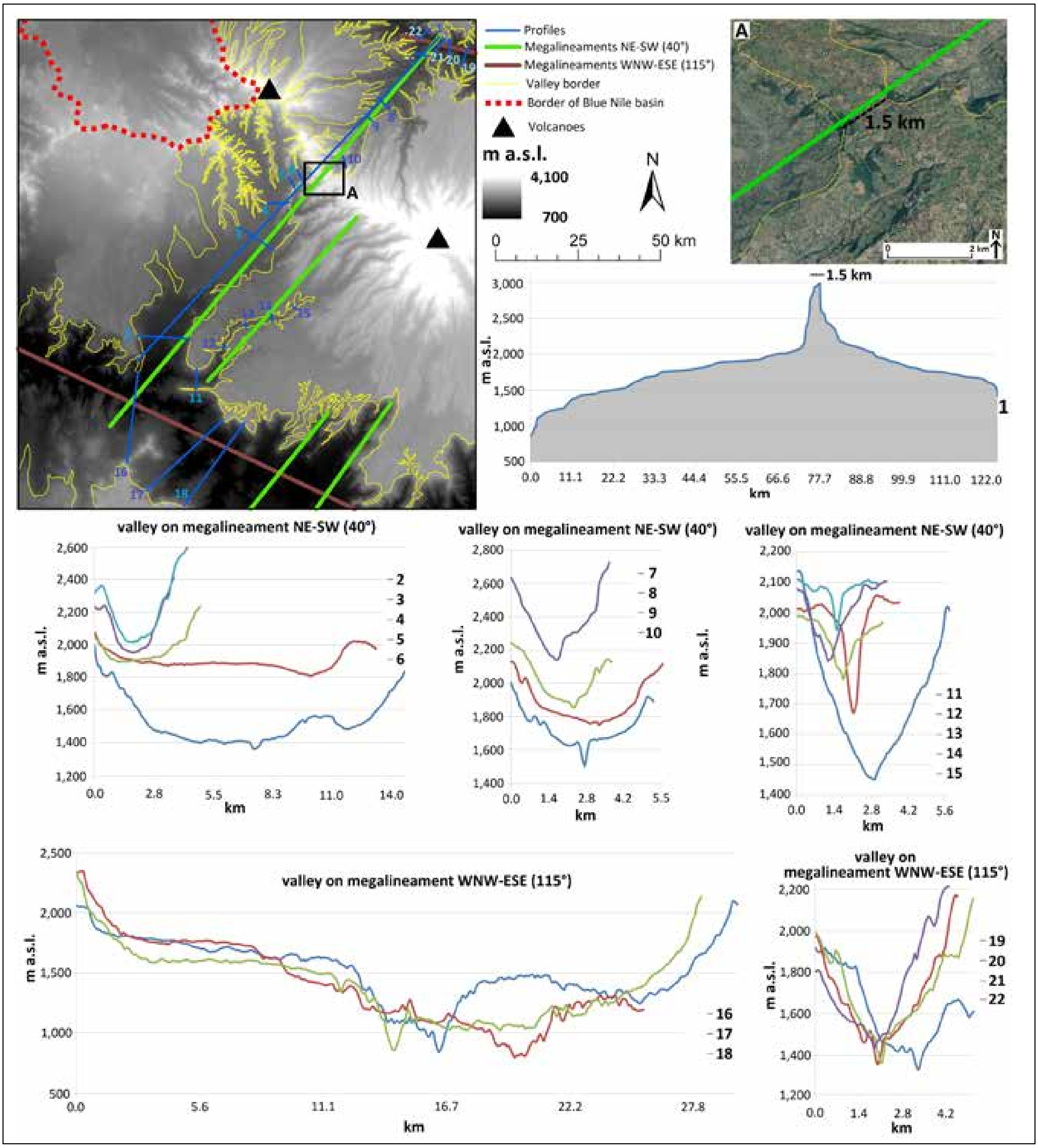

Fig. 10 Profiles in the Mt. Choke and Mt. Gish volcano sub-region. Note: Profile 1 along the single green line (an area with a tendency for river piracy); Profiles 2–15 are cross-sectional profiles directed across the valley and marked by green lines; Profiles 16–22 are cross-sectional profiles directed across the valley and marked by brown lines.

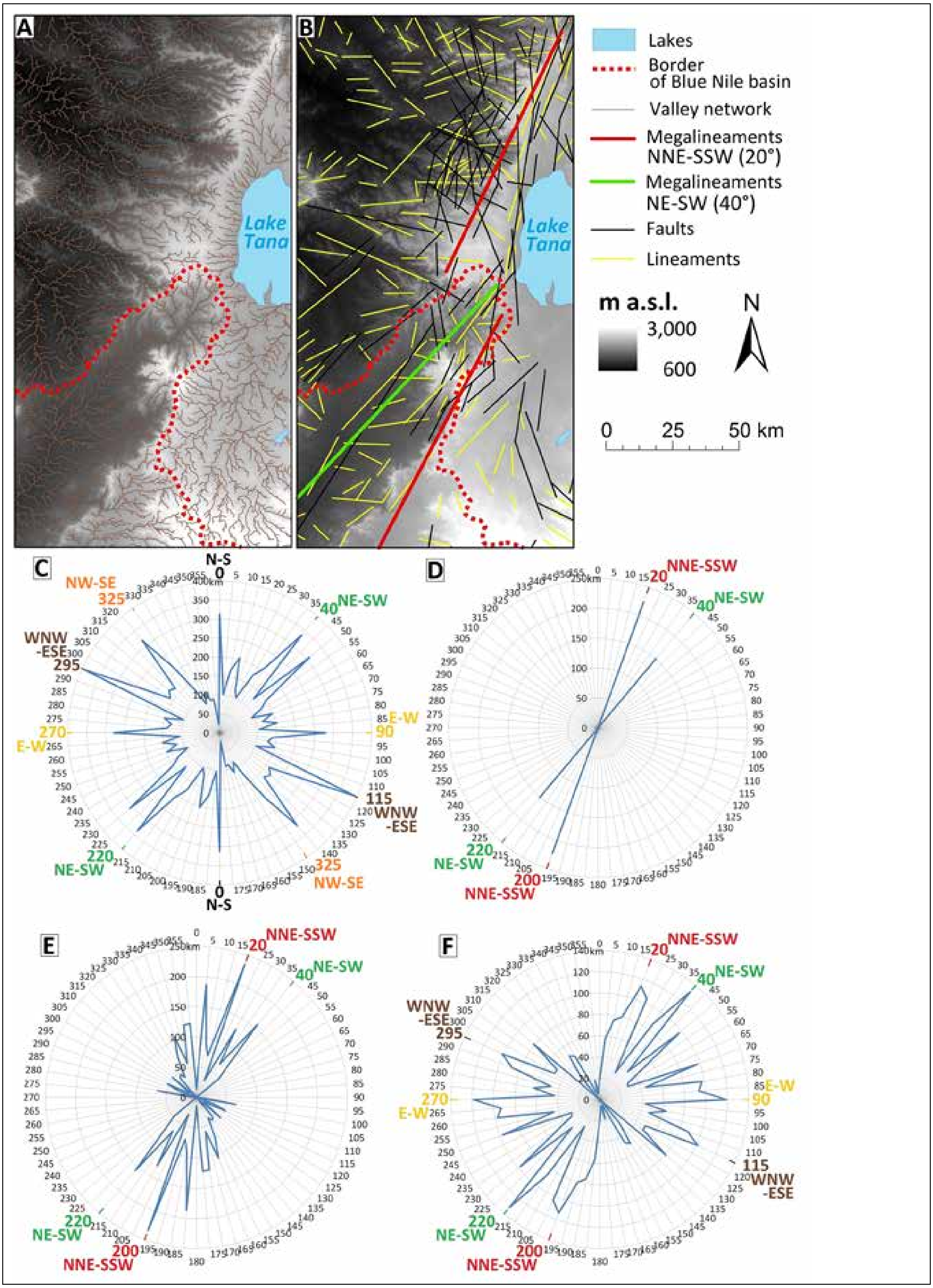

Fig. 11 Sub-region 4 (Lake Tana sub-region): A) map of the valley network and valley border; B) map of megalineaments, faults and lineaments; C) rose diagram of valley network azimuths; D) rose diagram of mega-lineamentsazimuths; E) rose diagram of fault azimuths (E); rose diagram of lineament azimuths (F).

seems to be dominant in the area of Mt. Choke and Mt. Gish, even though the river network should have a radial character around the volcanos. If we consider the fact that the NE-SW valleys (green lines) also cut 10.7 Ma old basalts, then they have to be younger than the basalts itself.

Another example of a tendency for river piracy was identified here (Figure 10A). Less than 1.5 km of the original landscape was left before the rivers from the SW or NE came across the old lava flows. Here we can presume expansion of a SW valley due to the profile (Fig. 10, profile 1).

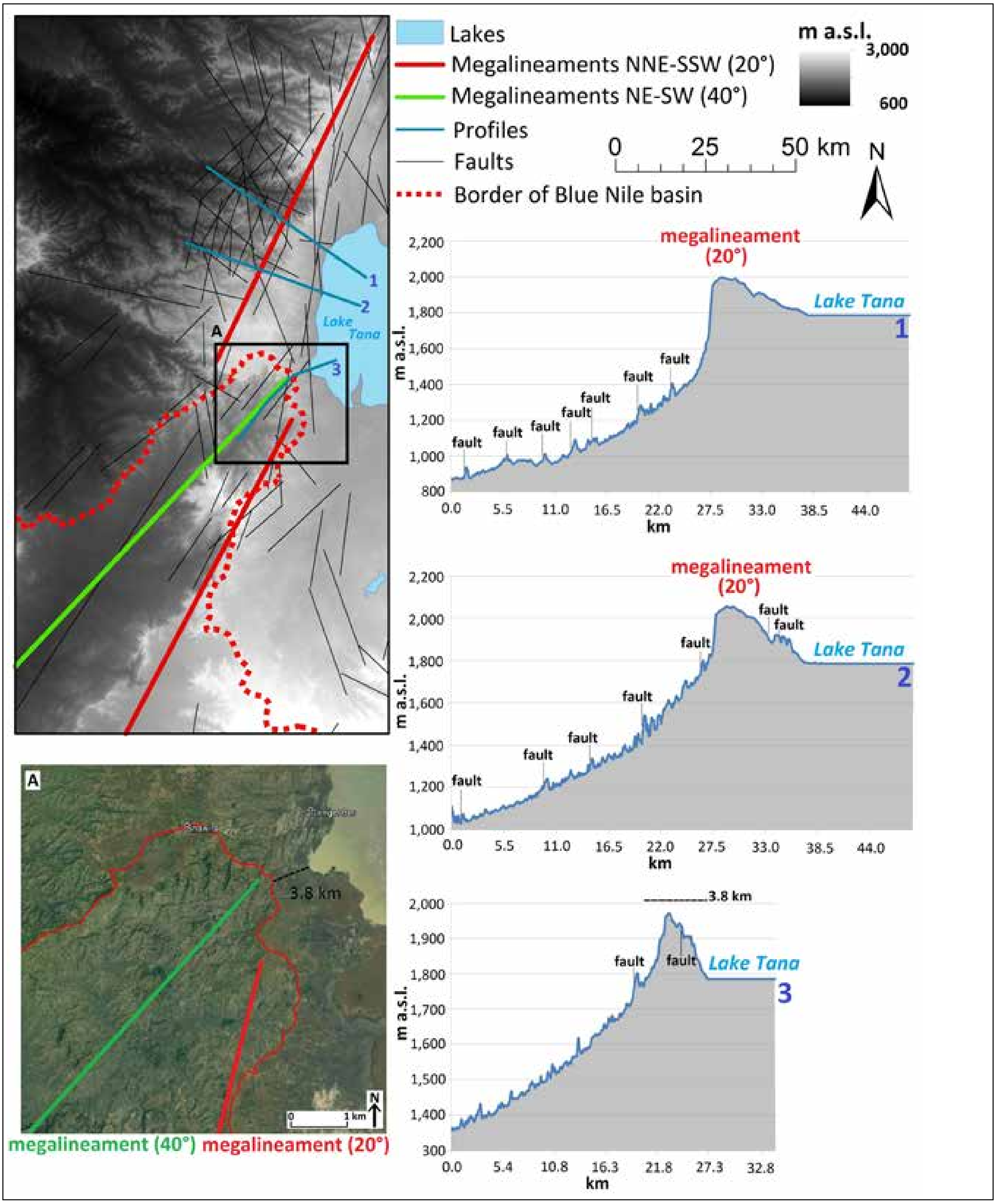

Fig. 12 Longitudinal profiles in the Lake Tana sub-region: Longitudinal profiles 1 and 2 show the situation for rivers stretching WNW-ESE; Longitudinal profile 3 shows the situation for rivers stretching SW-NE.

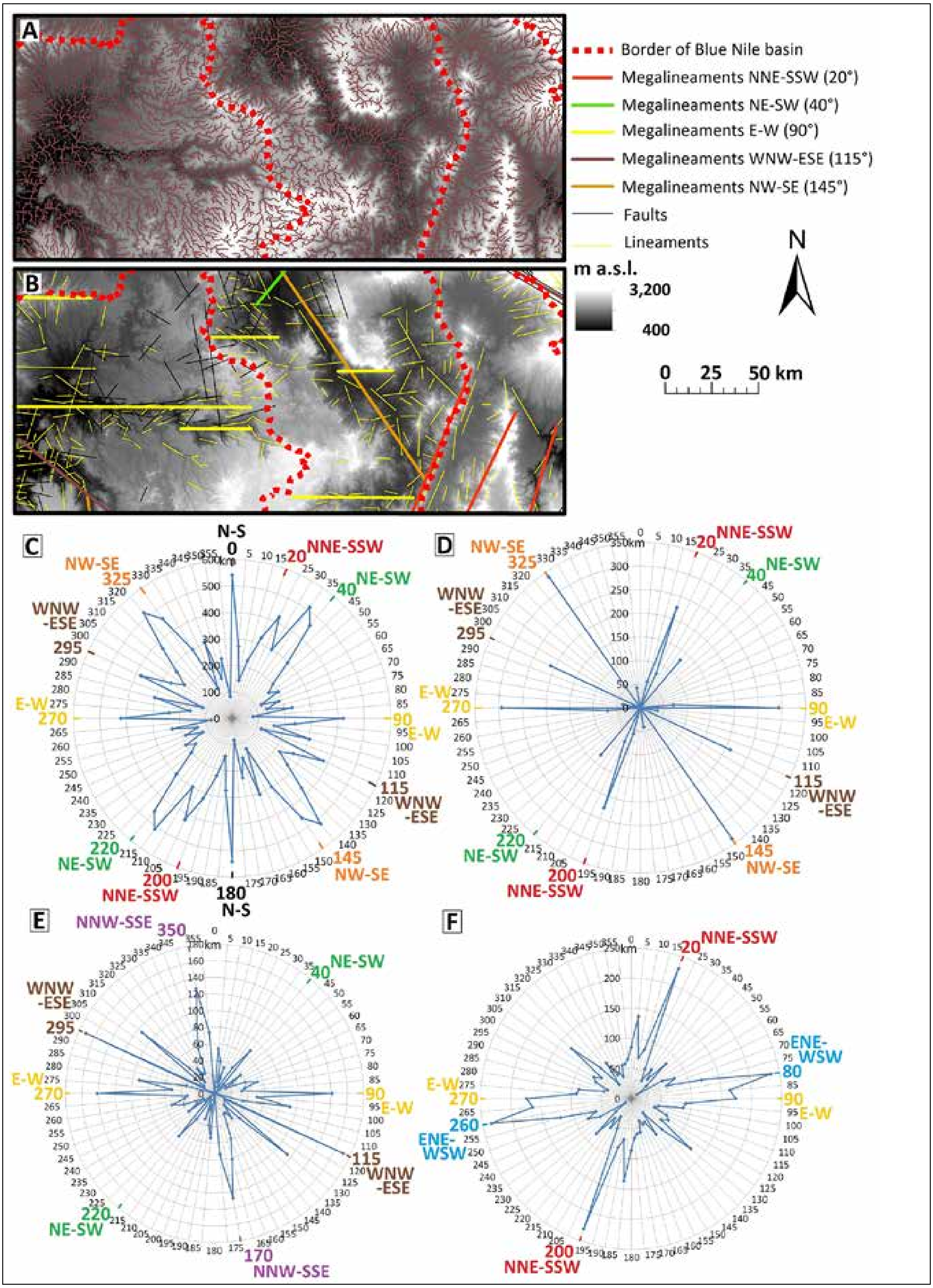

Fig. 13 Sub-region 5 (Didessa River and Baro River): A) map of the valley network and valley border; B) map of megalineaments, faults and lineaments; C) rose diagram of valley network azimuths; D) rose diagram of mega-lineamentsazimuths; E) rose diagram of fault azimuths (E); rose diagram of lineament azimuths (F).

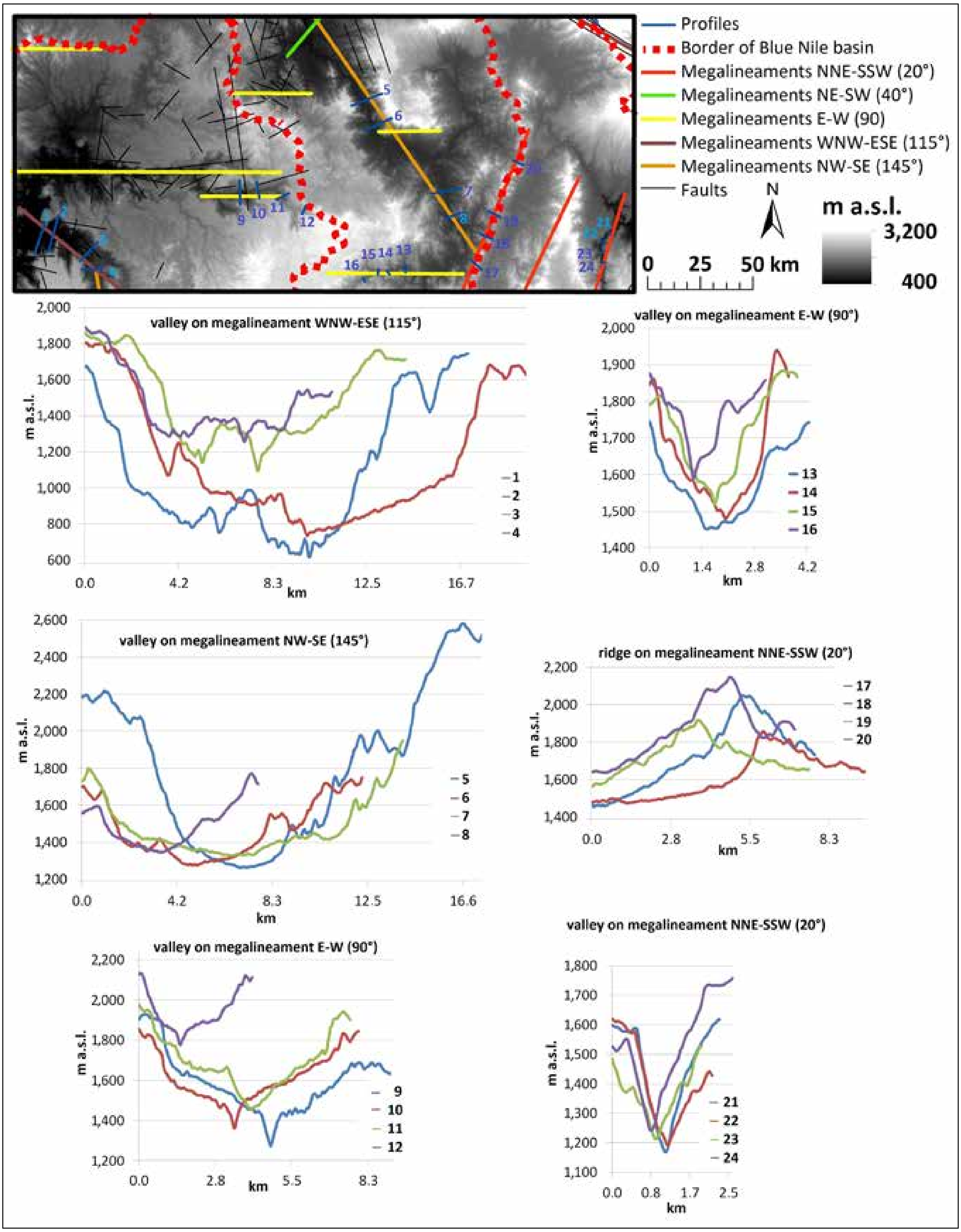

Fig. 14 Profiles in the Didessa River and Baro River sub-region. Note: Profiles 1–4 are cross-sectional profiles directed across the valley marked by a brown line; and profiles 5–8 are cross-sectional profiles directed across the valley marked by an orange line. Profiles 9–16 are cross-sectional profiles directed across the valley marked by a yellow line. Profiles 17–24 are cross-sectional profiles directed across the valley and ridge marked by a red line.

4.2.4 Lake Tana

The valley network seems to be only partly influenced by tectonics, namely in a NNE-SSW direction (azimuth of 20°). The valleys trending WNW-ESE (azimuth of 115°) do not show any connection to the mapped faults and are significant for the area to the west of the Lake Tana Basin. Nevertheless, both directions are marked because they represent a serious potential for river piracy (see the paragraph below). No significant recent erosional activity can be shown in a NNE-SSW direction (red lines), like in other sub-regions closer to the MER. It seems that the influence of the MER is not well pronounced in this part of the Ethiopian Highlands. Nevertheless, NNE-SSW faults exist in this area, and they influence both the lineaments and the megalineaments.

The whole of the Lake Tana Basin, which is tectonically predisposed (e.g. Chorowicz et al. 1998), now drains into the Blue Nile to the SE. Rivers on the western margin of the basin are approaching the lake due to headward erosion from two different directions (Figure 12). Longitudinal profiles 1 and 2 in Fig. 12 show the situation for rivers stretching WNW-ESE (brown lines on the rose diagram in Figure 11). The headwaters are approximately 10 km away from the lake; however, the headward erosion has to remove a 200 m high crest (escarpment) forming the lakeshore in the west (Sembroni et al. 2016). Another situation in the SW of the lake shows, river piracy taking place in a SW to NE direction (along the green lines) and the remnant, which must be crossed, is only 3.8 km long. Headward erosion along this green line is more probable because it is predisposed by the fault. The landscape on the lakeshore is also flatter and is created by a 150-m high remnant of lava flow from Mt. Gish (2,890 m a.s.l.).

Currently, the area of the Blue Nile basin covers 175,400 km^2 (between Lake Tana and the Roseires water reservoir). However, when Lake Tana will change the drainage to the SW, the cut off part of the Blue Nile Basin (98,600 km^2) will not be supplied by water from Lake Tana, but only by precipitation, which is not evenly distributed during the year. The annual rainfall in the Ethiopian Highlands is 1,800 mm and 80% of this precipitation falls from July to September (Klimadiagramme weltweit 2016).

4.2.5 Didessa River and Baro River

Many of the valleys (Figure 13) follow either a NW-SE or NE-SW direction where the valley bottoms are

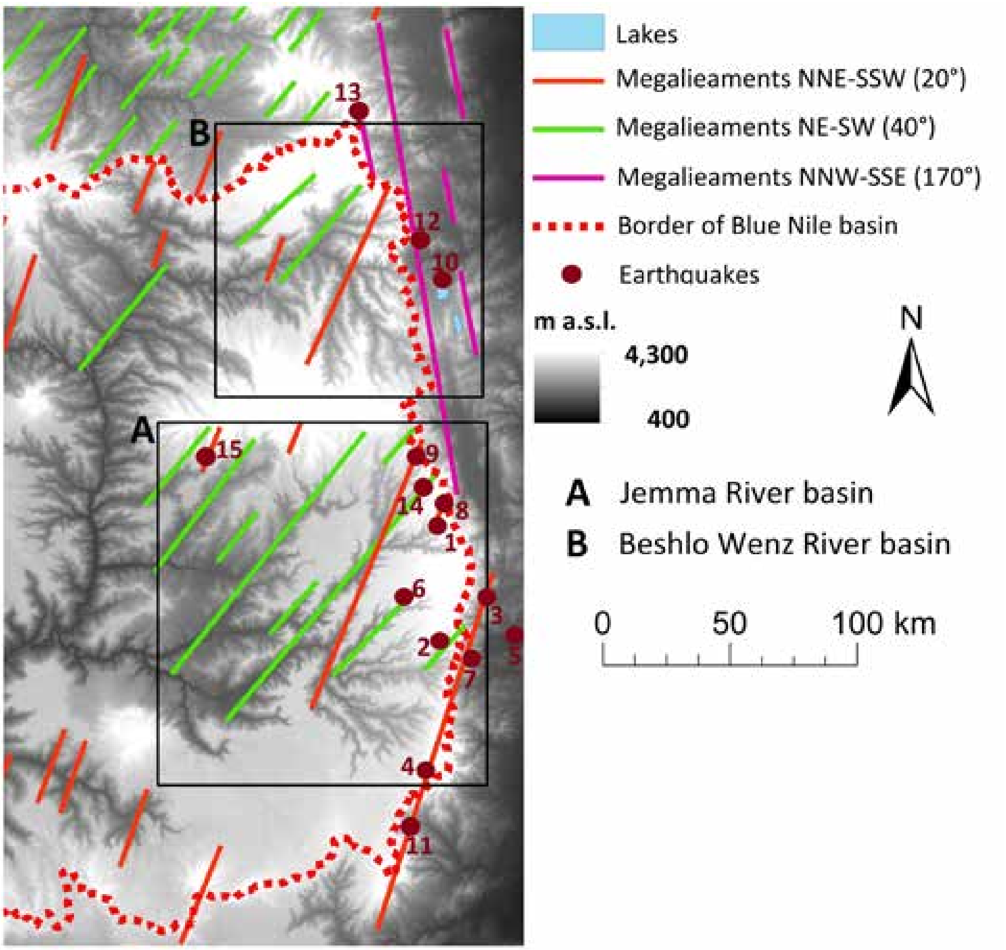

Fig. 15 Earthquake epicentres in the Jemma River Basin (A) and in the Beshlo Wenz Basin (B) (Earthquake Track 2017).

wider, which suggests an older river network. If we check the cross-sectional profiles (1–8) that stretch across brown and orange lines (azimuth 115° and 145°, respectively), the shapes resemble wide and open valleys (Figure 14). In addition, they are rather deep, which suggests a long period of evolution. A slightly different situation can be observed on the profiles crossing the yellow lines, whereby young erosion is already visible on the valley bottoms. An opposite situation to these valley profiles can be found in the valleys depicted by the red lines (profiles 21–24 in Fig. 14), which are again very deep, young and narrow (similar to Figure 7). The area of the Didessa and Baro rivers seems to be older in the sense of the evolution of the valley network with young erosion in the direction of the red lines (azimuth 20°).

4.3 Analysis of earthquake epicentres

A total of 12 earthquakes have occurred in and around the Jemma River Basin since 1961 (Figure 15A; Earthquake Track 2017). Most of the epicentres relate to "red lines" (eight events), only three to "green lines". In the Beshlo Wenz Basin (Figure 15B) the epicentres are located on faults with an azimuth of 170° (NNW-SSE orientation) depicted by a violet colour. This is due to a logical influence of the MER in this catchment. The average depth of the hypocentres is 20 km, which indicates rather shallow earthquakes and the average magnitude is 5.5.

4.4 Features of Guder River and Muger River network reorganisation

Features of drainage network reorganization along lineaments of various types can be detected in various parts of the Blue Nile Basin. The drainage networks of the Guder and Muger catchments (Figure 1*A*, Figure 16) are organised dominantly along diagonal green and orange lines; however, the most active recent river incision is along axial lines (yellow, violet, black and red, see Figure 16). This activity is evident mainly in lower parts of both watersheds as well as in the adjacent part of the Blue Nile valley. On the other hand, valleys along diagonal lines are wider, more denuded and are partly abandoned. A set of highly elevated depressions (2,600–3,000 m a.s.l.) elongated in a NNW-SSE direction (orange lines) can be identified on the southern watershed to the NW of Addis Ababa. Their very flat and wide bottoms (too large for the

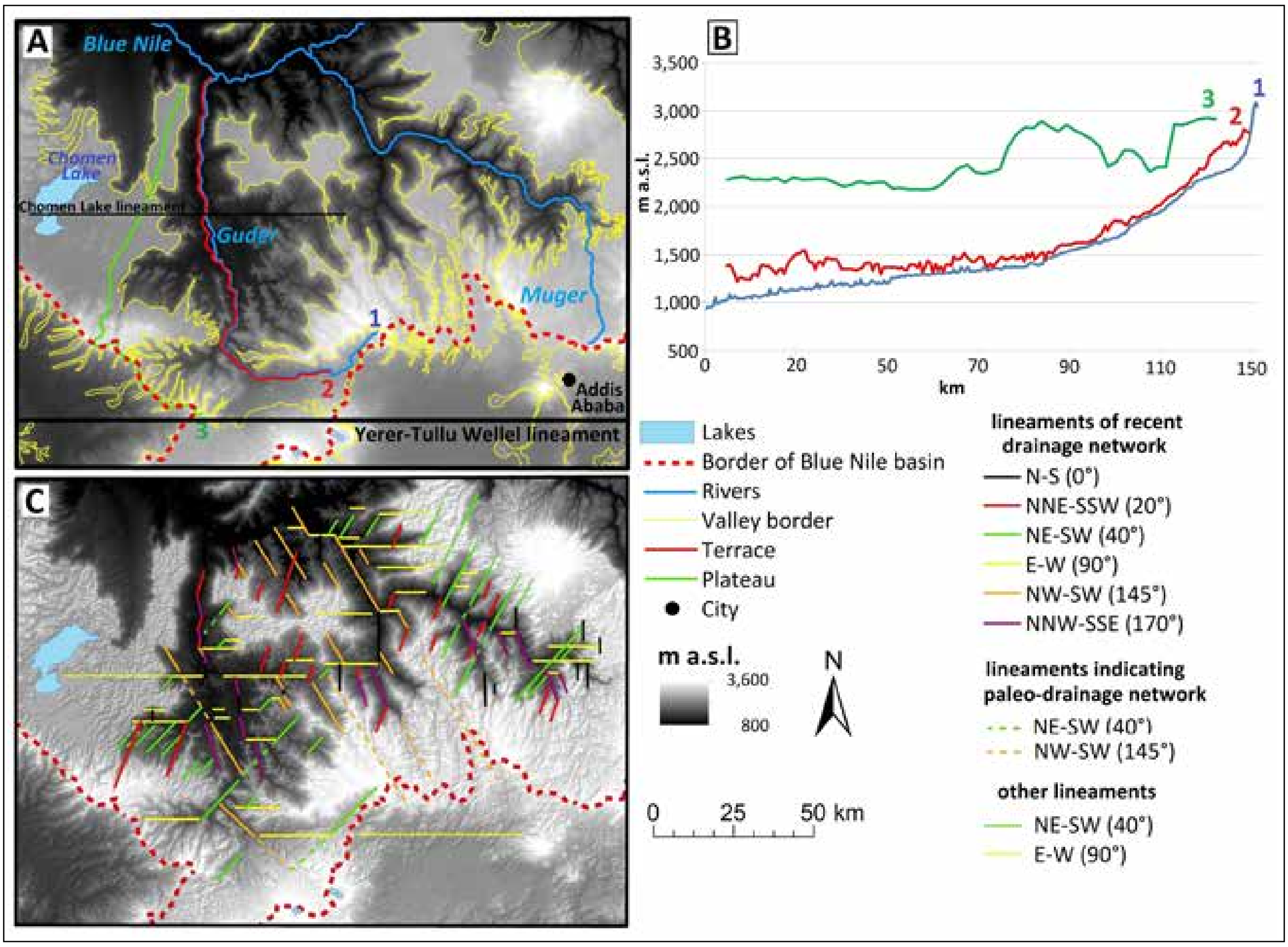

Fig. 16 The Sub-region A (Guder River and Muger River basin sub-region): A) Guder River and Muger River networks organised dominantly along diagonal green and orange lines; B) Profiles of Guga river (1), terrace (2) and plateau (3); C) lineaments of recent drainage network, lineaments indicating paleo-drainage network and other lineaments.

recent small streams) with differing descent (partly to the S and partly to the N) suggest that they belong to an ancient drainage network that might have drained the area towards the SE.

More detailed features of river network reorganisation can be seen in the longitudinal profile of the Guder River (Figure 16B). The river recently rose on the border scarp of the E-W oriented Yerer-Tullu Wellel lineament, below one of the above-mentioned paleo-valleys at an elevation of approximately 3,000 m a.s.l., where only several hundred horizontal meters are missing in order to capture the stream of the paleo-valley by headward erosion. Leaving the scarp, the river flows along the N boundary of the lineament without any notable incision. At an elevation of ~1,800 m a.s.l. it turns to the NW, where it flows across a denuded border scarp in a 0.5 km deep stepped canyon with a small decrease in gradient. The profile only becomes steeper when it crosses the W-E lineament to the east of Lake Chomen and then before it flows into the Blue Nile at an elevation of approximately ~950 m. Along with the typical character of the upper part of the profile, several other morphological features point to reverse flow of the river in the past. The general trend of the plateau inclination (from N to S) has been reversed by a strong uplift of the border of the Yerer-Tullu Wellel lineament (Figure 16); therefore, natural drainage to the S could have existed in the past. The strongly eroded, wide and branched middle part of the watershed contrasts with the narrow lower part closed between well preserved remnants of the volcanic plateau in the north. On the contrary, the uplifted plateau is markedly denuded in the south.

Probably the most interesting feature is the character of a wide terrace (2 in Figure 16B), which is directly incised by the river. The elevation of the terrace rises from the mouth (~1,350 m a.s.l.) only approximately 20 km (~1,450 m a.s.l.) to the narrowest part of the valley bounded by remnants of the plateau. Subsequently (from 20 km to 70 km), the terrace is reversed to recent river as for W-E elevated belt at Lake Chomen lineament. Nevertheless, a small paleo-valley on the southern border sloping to the S is also an indication of reverse flow here. Further to the S, the river is not incised and probably flows down to the terrace (~1,300 m a.s.l.) to the point where a general rise in the elevation of the plateau begins (Figure 16). The former water shed divide, approximately 20 km from the recent mouth, and at least a 50 km long reversed flow of the river can be inferred. Considering all other indices, drainage towards the SSE, mainly along diagonal lines, can be assumed before the uplift of the border of the Yerer-Tullu Wellel lineament. Therefore, reorganization of the drainage network in relation to the current situation took place later by headward erosion, mainly along the axial lines.

5. Discussion

Landscape analysis from SRTM DEM data is of great interest to geoscientists (e.g. Martino et al. 2009; Haider et al. 2015). SRTM DEM data are often used for three types of morphometric analysis: discrete elevation function *f* (x, y, z), hill shading as well as flow direction and flow accumulation. All three were also very useful for performing a morphostructural analysis of the upper Blue Nile Basin and its surroundings.

Hill shading offers many possibilities for interpreting detailed surface structures that are often completely imperceptible using simple DEM visualization (e.g. Kennelly 2008). Hill shading allowed us to perform a much more accurate delineation of lineaments and borders of erosion than mapping from certain satellite images only (Kusák et al. 2016). However, the overlapping of layers (the digital elevation model; hillshade images of various elevation angles of the illumination source and the solar azimuths; satellite images with a pixel size of 15 m placed on the virtual globe of Google Earth) proved to be the most useful when checking the manually mapped landscape shapes (following Wladis 1999; Ehlen 2004; Gani and Abdelsalam 2006). Morphometric analysis based on a calculation of the potential drainage of each pixel of an SRTM DEM shows the shape, density and hierarchy of valley networks, which reflect the influence of structure and erosion processes on the formation of the landscape (*sensu* Stoddart 1997; Kusák et al. 2016), similarly to an evaluation of various topographic profiles. A set of all of these analyses was effectively used in the central part of the area by Gani and Abdelsalam (2006) but our work brings a different type of information.

The character of faults, their direction and space differentiation as well as time of formation and reactivation, are important for the reconstruction of the morphotectonic development. However, direct investigation of faults is limited to outcrops, boreholes and geophysical profiles, which is time demanding. Therefore, they are not mapped equally in detail on geological maps and the distinction of their origin and activation is limited. On the other hand, lineaments reflecting the geological fractures can only be uniformly mapped with a certain probability on the basis of a DEM. Mega-lineaments are most probably connected with important faults, but because of their limited number they are not as suitable for statistical analysis as regular lineaments. The stages of development of structurally determined landforms can also be estimated from topographic profiles and the presence of morphodynamic phenomena (erosion, landslides, earthquakes) (Gani and Neupne 2018). Finally, the combined information from all of these sources can be compared to the results of various geological and geochronological analyses to obtain a comprehensive picture of the morphotectonic development.

Two basic groups of structural features can be distinguished based on our analysis of the upper part of the Blue Nile basin:

a) Axial (including black, yellow, violet, blue and red lines) around N-S and E-W directions.
b) Diagonal (including green, orange and brown lines) around NE-SW and NW-SE directions.

The difference between the red and green lines (representatives of the basic groups mostly contained in the faults and lineaments) is associated with a transition from a 130°E-oriented extension to a 105°E-oriented extension of the MER sometime between 6.6 to 3 Ma ago, which caused a change in the normal fault orientations from predominantly N35°E to N10°E (Wolfenden et al. 2004). The diagonal features also reflect yet older development of the Blue Nile Basin, i.e. its formation as a NW-trending rift (Gani et al. 2009; MacGregor 2015). Axial features mainly respond to Quaternary development, which is influenced by E-W and NNE-SSW-oriented extensions related to an oblique opening of the MER and development of E-trending transverse faults as well as E-W-oriented extensions in western Afar (Gani et al. 2009). Landslides linked with axial directions confirm Quaternary activity too (Kycl et al. 2017).

The young Quaternary character of the majority of the axial lines was also confirmed by our analyses. They are characterized by prevailing deep and narrow valleys, fault scarps, earthquake activity and a tendency for recent river piracy. On the contrary, the diagonal lines are generally linked with wider and more open valleys with a higher tendency for meandering or braided channels, a dominant abundance of higher order streams and significant "well-developed" relief features. Reorganisation of the drainage networks of the Guder and Muger rivers from the diagonal to axial directions supports this dichotomy.

The development of lineaments and river networks is generally accelerated by the uplift of the area. The initial Paleogene surface of the volcanic plateau of the Ethiopian Highlands probably formed at elevation significantly lower than now, and then had been decreasing until the Late Miocene (MacGregor 2015). Indeed, Pike et al. (2003) suggest that erosion initiated in the Blue Nile canyon as early as 25–29 Ma ago, but Gani et al. (2009) evaluated only a very gentle incision rate of the Blue Nile up to the Late Miocene, whereas rapid erosion would have started only 6 Ma ago. Generally, the neotectonic uplift of the territory can be connected with the opening of the MER (11 – 6 Ma ago according to various authors – c.f. Gani et al. 2009; Ismail and Abdelsalam 2012) but uplift of the Lake Tana sub-region probably began earlier, i.e. before the end of the mid-Tertiary flood volcanism when the asthenospheric mantle intruded the lithosphere as a result of plume activity, inducing thermal uplift (Chorowicz et al. 1998). Further an initial radial drainage network could have formed including outflow to the S (see section 4.4), which was later blocked by Late Miocene and Pliocene tectono-thermal uplift of the MER shoulders and relative subsidence of the Tana basin (Chorowicz et al. 1998; Sembroni et al. 2016). We can speculate that in this initial stage the upper part of the Blue Nile could have also drained along the ancient NW-SE (orange) or WNW-ESE (brown) structures to the area of the recent Afar depression. An indication of this may be the mature erosional pattern of the E and SE part of the Blue Nile Basin in comparison with the more homogeneous (younger) erosional pattern of the W and SW parts (Gani and Abdelsalam, 2006) and also indications of diagonally-elongated palaeovalleys in the recent watershed around the city of Dessie.

The spatial distribution of the particular types of the studied linear features can be linked with the time-space character of the background tectonic events. Sub-region 1 lies closely westward of the MER, and sub-region 2 directly on the border of the Afar depression. Sub-regions 3 and 4 are far from the rift boundary and the eastern part of sub-region 5 is close to the Rift (Figure 1). The investigated (coloured) directions represent only 44% of the possible drainage courses. Nevertheless, 62% (sub-region 4) to 87% (sub-region 2) of the drainage agrees with the analysed directions. This not only confirms the significant influence of tectonics on the drainage network, but also an increase in this influence around the boundary of the MER and in particular the Afar depression. Axial directions dominate in sub-regions near or on the rift boundary (sub-regions 1, 2 and 5), whereas diagonal directions are comparably significant only in the last two sub-regions.

The brown direction is mainly about the SW part of sub-regions 3 and 5 with the most mature relief and exposed pre-Tertiary bedrock, which suggests its ancient character. The orange direction has a similar character, but its important representation in sub-region 2 and the eastern part of sub-region 5 suggest neotectonic reactivation (Abebe et al. 1998). The green direction is generally the most represented in all of the linear features, mainly in sub-regions 1, 3 and 4. Transformation of tectonic failures into the drainage network indicates the oldest neotectonic event of regional significance, i.e. opening of the MER.

The red lines are second in the order of areal importance (after the green lines) and are connected with the stress field of the MER, but are less pronounced in the inner part of the Ethiopian Highlands. The black and violet lines have only a limited areal influence on the adjacent parts of the MER and Affar (their higher importance was revealed only in sub-region 2), while they are the youngest and have been active for the short period of time. The yellow lines are located in the south of the upper part of the Blue Nile Basin and they are primarily a result of activation of the Yerer-Tullu Wellel lineament in the Late Miocene. Nevertheless, recessing the lower parts of their cross profiles means that the Quaternary tectonic activity increases in an E-W direction.

The Ethiopian Highlands are one of the most tectonically influenced areas in the world (Beyene and Abdelsalam 2005; Gani et al. 2007, 2009), so river erosion and river piracy are very active there. The valley networks are young and water divides change position easily. Thanks to the steeper slopes and a more humid climate inside the MER, the water courses (tributaries of the Awash River) have more erosive power and the Jemma and Beshlo Wenz river basins lose parts of their catchments as the water divide is moving slightly towards the west (Kusák et al., 2016). However, the most significant effect of river piracy would probably be seen in the Lake Tana Basin.

Currently, the Lake Tana Basin is in the focus of many scientific disciplines in terms of: 1) geology and geochronology (Prave et al. 2016); 2) reproducing historic sediment concentrations (Kabaa et al. 2014); 3) chemical analysis of water and sediment (Ahrens et al. 2016); 4) assessing the implications of water harvesting intensification on upstream–downstream ecosystem services (Dile et al. 2016); etc.. All of the above stated research activities and many other authors write about the Lake Tana Basin as a single unit, but do not include the processes taking place in the surroundings. River piracy approaches the Lake Tana Basin from SW to NE (along the green lines) and the remnant, which has to be surpassed, is only 3.8 km long (Figure 12). The potential change of drainage of Lake Tana to the SW (instead of to NE) will greatly influence the hydrological conditions over a rather large area.

6. Conclusion

The results of simple morphostructural analysis from a DEM can be interpreted in high concordance with the present results of stratigraphic, structural, petrologic, tectonic and geochronologic investigations of the Ethiopian Highlands. The azimuths of lineaments, faults and river networks combined with erosional features, cross-sectional and longitudinal valley profiles reveal a change in the dominant stress fields and stages of topography development.

The NW-SE (orange lines) and WNW-ESE (brown lines) linear features correspond with older stress fields organizing the formation of ancient pre-Neogene rifts and transposed onto the volcanic plateau during the first phases of its rise. They probably determined a palaeo-drainage system that could partially flow to the south and east across the recent rift shoulders and are well pronounced in sub-regions with uncovered pre-volcanic bedrock. These directions are characterized by extremely braided valleys with locally brained channels, small remnants of volcanic plateau and features of well-developed relief'. They are typical for the oldest part of Blue Nile and Didesa valley.

The beginning of the neotectonic stage (during which the modern topography and drainage network formed) can be connected to the opening of the MER during the Late Miocene. The most wide-spread NE-SW (green) linear features parallel to MER represent the long term morphotectonic influence of an NW-SE extension in the whole territory. Reactivation of some NW-SE (orange) linear features mainly near the MER boundary match with activity of the offset faults. Developed (wider, more open) valleys and more 'mature relief' are typical for the leading green direction.

Pliocene counter clockwise rotation of the MER stress field led (mainly in the MER surrounding) to the generation of NNE-SSW (red) linear features. The stress field transition was linked also with intensive uplift of the whole territory, especially the rift shoulders that definitely blocked any existing outflow toward S or E. Continuing relative subsidence of the Lake Tana basin, headward erosion and river piracy could contribute to spreading of the Blue Nile basin too. Morphological features such as incised narrow valleys, indices of river piracy, valley asymmetry and the generally 'young age relief' characteristic for the red direction support this interpretation.

N-S (black and violet) linear features represent the youngest Quaternary development of the territory connected with E-W extension in MER and western Afar. They are morphologically least developed and represented by huge fault slopes with tectonic blocks and active youngest upper parts of valleys. Orthogonal features with E-W direction are dominant along older (Late Miocene) Yerer-Tullu Wellel volcanotectonic lineament, however they show evident features of recent reactivation in cross profiles and tendency to river piracy. Accelerating Quaternary uplift created recent very high relief mainly along the boundary with MER and Afar depression and so conditions for intensive headward erosion from the outside the Blue Nile basin that could lead to its reduction by river piracy in the near future.

Acknowledgements

The study was supported by the GACR project "Mass wasting and erosion as an indicator of morphotectonic activity in the Ethiopian Highlands based on remote sensing approaches" (P209/12/J068) and by the Grant Agency of Charles University in Prague, Czech Republic "Morphostructural analysis of Ethiopian Highlands based on remote sensing" (1436314). Jozef Minár was supported by the Slovak Research and Development Agency under the contract No. APVV-15-0054. The SRTM DEM was provided by the U.S. Geological Survey. This work was carried out thanks to support of the long-term conceptual development research organization RVO: 67985891. We wish to thank Craig M. Hampson and Frederick Rooks for language editing.

References

Abdullah, A., Akhir, J.M., Abdullah, I. (2010): Automatic Mapping of Lineaments Using Shaded Relief Images Derived from Digital Elevation Model (DEMs) in the Maran – Sungi Lembing Area. Malaysia. EJGE 15, 949–957.

Abebe, T., Mazzarini, F., Innocenti, F., Manetti, P. (1998): The Yerer-Tullu Wellel volcanotectonic lineament; a transtensional structure in central Ethiopia and the associated magmatic aktivity. Journal of African Earth Sciences 26(1), 135–150, https://doi.org/10.1016/S0899-5362(97)001413.

Ahrens, L., Gashaw, H., Sjoholm, M., Gebrehiwot S. G., Getahun, A., Derbe, E., Bishop, K., Åkerblom, S. (2016): Poly- and perfluoroalkylated substances (PFASs) in water, sediment and fish muscle tissue from Lake Tana, Ethiopia and implications for human exposure. Chemosphere 165, 352–357, https://doi.org/10.1016/j.chemosphere.2016.09.007.

Ayalew, L., Yamagishi, H. (2003): Slope failures in the Blue Nile basin, as seen from landscape evolution perspective. Geomorphology 57(1–2), 95–116, https://doi.org/10.1016/S0169-555X(03)00085-0.

Ayman, A. A., Abdelkareem, M., Asran, A. M., Mahran, T. M. (2017): Geomorphic and lithologic characteristics of Wadi Feiran basin, southern Sinai, Egypt, using remote sensing and field investigations. Journal of Earth System Science 126(85), 1–25, https://doi.org/10.1007/s12040-017-0861-8.

Belisario, F., Del Monte, M., Fredi, P., Funiciello, R., Palmieri, E. L., Salvini, F. (1999): Azimuthal analysis of stream orientations to define regional tectonic lines. Zeitschrift für Geomorphologie Supplementary Issues 118, 41–63.

Beyene, A., Abdelsalam, M. G. (2005): Tectonics of the Afar Depression: A review and synthesis. Journal of African Earth Sciences 41(1–2), 41–59, https://doi.org/10.1016/j.jafrearsci.2005.03.003.

Chorowitz, J. (2005): The East African rift system. Journal of African Earth Sciences 43(1–3), 379–410, https://doi.org/10.1016/j.jafrearsci.2005.07.019.

Chorowicz, J., Collet, B., Bonavia, F. F., Mohr, P., Parrot, J. F., Korme, T. (1998): The Tana basin, Ethiopia: Intra-plateau uplift, rifting and subsidence. Tectonophysics 295(3–4), 351–367, https://doi.org/10.1016/S0040-1951(98)00128-0.

CiotolI, G., Seta, M. D., Del Monte, M., Fredi., P., Lombardi, S., Palmieri, E. L., Pugliese, F. (2003): Morphological and geochemical evidence of neotectonics in the volcanic area of Monti Vulsini (Latium, Italy). Quaternary International 101–102, 103–113, https://doi.org/10.1016/S1040-6182(02)00093-9.

Dile, Y., T., Karlberg, L., Daggupati, P., Srinivasan, R., Wiberg, D., Rockströmd, R. (2016): Assessing the implications of water harvesting intensification on upstream-downstream ecosystem services: A case study in the Lake Tana basin. Science of the Total Environment 542(part A), 22–35, https://doi.org/10.1016/j.scitotenv.2015.10.065.

Ehlen, J. (2004). Lineation. In Goudie, A. S. (ed.) et al.: Encyclopaedia of geomorphology. Routledge, London, 623–624.

Earthquake Track [online]. [downloaded 10/01/2017]. www.earthquaketrack.com.

ESRI Inc. ArcMap™. Ver. 10.1. Copyright 2015. [online]. [downloaded 01/01/2015]. www.esri.com.

Gani, N., D., Abdelsalam, M. G. (2006): Remote sensing analysis of the Gorge of the Nile, Ethiopia with emphasis on Dejen-Gohatsion region. Journal of African Earth Science 44, 145–150, https://doi.org/10.1016/j.jafrearsci.2005.10.007.

Gani, N. D., Gani, M. R., Abdelsalam, M. G. (2007): Blue Nile incision on the Ethiopian Plateau: Pulsed plateau growth, Pliocene uplift, and hominin evolution. GSA Today 17, 4–11, https://doi.org/10.1130/GSAT01709A.1.

Gani, N. D., Abdelsalam, M. G., Gera, S., Gani, M. R. (2009): Stratigraphic and structural evolution of the Blue Nile Basin, Northweastern Ethiopian Plateau. Geological Journal 44(1), 30–56, https://doi.org/10.1002/gj.1127.

Gani, N. D., Neupane, P. C. (2018): Understanding transient landscape of the Ethiopian Plateau in relation to mantle dynamics. Geological Journal 53(1), 371–385, https://doi.org/10.1002/gj.2903.

Google Earth, Google Inc. Available from URL. [online]. [downloaded 01/01/2015]. http://www.google.cz/intl/cs/earth

Haider, V. L., Kropáček, J., Dunkl, I., Wagner, B., and Von Eynatten, H. (2015): Identification of peneplains by multi-parameter assessment of digital elevation models. Earth Surface Processes and Landforms 40(11), 1477–1492, https://doi.org/10.1002/esp.3729.

Ismail, E. H., Abdelsalam, M. G. (2012): Morpho-tectonic analysis of the Tekeze River and the Blue Nile drainage systems on the Northwestern Plateau, Ethiopia. Journal of African Earth Sciences 69, 34–47, https://doi.org/10.1016/j.jafrearsci.2012.04.005.

Jenson S. K., Domingue, J. O. (1988): Extracting Topographic Structure from Digital Elevation Data for Geographic Information System Analysis. Photogrammetric Engineering and Remote Sensing 54(11), 1593–1600, http://citeseerx.ist.psu.edu/viewdoc/download?doi=10.1.1.138.6487andrep=rep1andtype=pdf.

Kaba, E., Philpot, W., Steenhuis, T. (2014): Evaluating suitability of MODIS-Terra images for reproducing historic sediment concentrations in water bodies: Lake Tana, Ethiopia. International Journal of Applied Earth Observation and Geoinformation 26, 286–297, https://doi.org/10.1016/j.jag.2013.08.001.

Kazmin, V. (1975): Geological Map of Ethiopia, Geological Survey of Ethiopia, Addis Ababa, Ethiopia.

Kennelly, P. (2008): Terrain maps displaying hill-shading with curvature. Geomorphology 102(3–4), 567–577, https://doi.org/10.1016/j.geomorph.2008.05.046.

Kieffer, B., Arndt, N., Lapierre, H., Bastien, F., Bosch, D., Pecher, A., Yirgu, G., Ayalew, D., Weis, D., Jerram, D. A., Keller, F., Meugniot, C. (2004): Flood and shield basalts from Ethiopia: Magmas from the African Superswell. Journal of Petrology 45(4), 793–834, https://doi.org/10.1093/petrology/egg112.

Klimadiagramme weltweit. [online]. [downloaded 10/10/2016]. www.klimadiagramme.de.

Koronovskya, N. V., Bryantsevaa G. V., Goncharova M. A., Naimarka A. A, Kopaev A. V. (2014): Lineaments, Planetary Jointing, and the Regmatic System: Main Points of the Phenomena and Terminology. Geotectonics 48(2), 151–162, https://doi.org/10.1134/S0016852114020058.

Kusák, M., Kropáček, J., SchillacI, C., Vilímek, V. (2016): Aspects of the evolution of the Jemma River basin in the Ethiopian Highlands determined by means of a relief analysis based on Digital Elevation Model (DEM), Ethiopia. Geografia Fisica e Dinamica Quaternaria 39, 37–50, https://doi.org/10.4461/GFDQ.2016.39.4.

Kusák, M., Krbcová, K. (2017): Analysis of the relationship of automatically and manually extracted lineaments from DEM and geologically mapped tectonic faults around the Main Ethiopian Rift and the Ethiopian Highlands, Ethiopia. AUC Geographica 52(1), 5–17, https://doi.org/10.14712/23361980.2017.1.

Kycl, P., Rapprich, V., Verner, K., Novotný, J., Hroch, T., Mišurec, J., Eshetu, H., Haile, E. T., Alemayehu, L., Goslar, T. (2017): Tectonic control of complex slope failures in the Ameka River Valley (Lower Gibe Area, central Ethiopia): Implications for landslide formation. Geomorphology 288, 175–187, https://doi.org/10.1016/j.geomorph.2017.03.020.

Macgregor, D. (2015): History of the development of the East African Rift System: A series of interpreted maps through time. Journal of African Earth Sciences 101, 232–252, https://doi.org/10.1016/j.jafrearsci.2014.09.016.

Mäerker M., Hochschild V., Maca V., Vilímek V. (2016): Stochastic assessment of landslides and debris flows in the Jemma basin, Blue Nile, Central Ethiopia. Geografia Fisica e Dinamica Quaternaria 39(1), 51–58, https://doi.org/10.4461/GFDQ.2016.39.5.

Mangesha, T., Chernet, T., Haro, W. (1996): Geological Map of Ethiopia (1 : 250,000). Geological Survey of Ethiopia: Addis Ababa, Ethiopia.

Martino, C., Nico, G., Schiattarella, M. (2009): Quantitative analysis of InSAR digital elevation models for identification of areas with different tectonic activities in southern Italy. Earth Surface Processes and Landforms 34(1), 3–15, https://doi.org/10.1002/esp.1681.

Minár, J., Sládek, J. (2008): Morphological network as an indicator of a morphotectonic field in the central Western Carpathians (Slovakia). Zeitschrift für Geomorphologie 53(2), 23–29, https://doi.org/10.1127/0372-8854/2009/0053S3-0023.

Pik, R., Deniel, C., Coulon, C., Yirgu, G., Hoffmann, C., Ayalew, D. (1998): The northwestern Ethiopian Plateau flood basalts: classification and spatial distribution of magma types. Journal of Volcanology and Geothermal Research 81(1–2), 91–111, https://doi.org/10.1016/S0377-0273(97)00073-5.

Pik, R., Marty, B., Carignan, J., Lavé, J. (2003): Stability of the Upper Nile drainage network (Ethiopia) deduces from (U/Th)/He thermochronometry: implications for uplift and erosion of the Afar plume dome. Earth and Planetary Science Letters 215(1–2), 73–88, https://doi.org/10.1016/S0012-821X(03)00457-6.

Pravea, A. R., Batesa, C. R., Donaldsona, C. H., Tolandb, H., Condonc, D. J., Markd, D., Rauba, T. D. (2016): Geology and geochronology of the Tana Basin, Ethiopia: LIP volcanism, super eruptions and Eocene-Oligocene environmental change. Earth and Planetary Science Letters 443, 1–8, https://doi.org/10.1016/j.epsl.2016.03.009.

Sembroni, A., Faccenna, C., Becker, T. W., Molin, P., Abebe, B. (2016): Long-term, deep-mantle support of the Ethiopia-Yemen Plateau. Tectonics 35(2), 469–488, https://doi.org/10.1002/2015TC004000.

Smith, M. J., Clark, C. D. (2005): Methods for the visualisation of digital elevation models for landform mapping. Earth Surface Processes and Landforms 30(7), 885–900, https://doi.org/10.1002/esp.1210.

Stoddart, D. R. (ed.) (1997): Process and form in geomorphology. Routledge, London.

Šilhavý, J., Minár, J., Mentlík, P., Sládek, J. (2016): A new artefacts resistant method for automatic lineament extraction using Multi-Hillshade Hierarchic Clustering (MHHC). Computers and Geosciences 92, 9–20, https://doi.org/10.1016/j.cageo.2016.03.015.

Ukstins, I. A., Renne, P. R. Wolfenden, E., BakeR, J., Ayalew, D., Menzies, M. (2002): Matching conjugate volcanic rifted margins: 40Ar39Ar chrono-stratigraphy of pre and syn-rift bimodal flood volcanism in Ethiopia and Yemen. Earth and Planetary Science Letters 198(3–4), 289–306, https://doi.org/10.1016/S0012-821X(02)005253.

U.S. Geological Survey [online]. [downloaded 10/01/2017]. www.usgs.gov.

Wladis, D. (1999): Automatic Lineament Detection Using Digital Elevation Models with Second Derivative Filters. Photogrammetric Engineering and Remote Sensing 65(4), 453–458, https://pdfs.semanticscholar.org/3c9e/4f7863002102ead6d390954ff4d1225e1f6d.pdf.

Wolela, A. (2010): Diagenetic evolution of the Ansian-Pliensbachian Adigrat Sandstone, Blue Nile Basin, Ethiopia, Journal of African Earth Science, 6 (1), 29–42, https://doi.org/10.1016/j.jafrearsci.2009.05.005.

Wolfenden, E., Ebiger, C., Yirgu, G., Deino, A., Ayalew, D. (2004): Evolution of the northern Main Ethiopian Rift: birth of a triple junction. Earth and Planetary Science Letters 224(1–2), 213–228, https://doi.org/10.1016/j.epsl.2004.04.022.